Viscoelasticity of Concentrated Isotropic Solutions of Semiflexible Polymers. 2. Linear Response

David C. Morse

Department of Chemical Engineering and Materials Science, University of Minnesota, 421 Washington Avenue S.E., Minneapolis, Minnesota 55455

Received February 25, 1998; Revised Manuscript Received July 2, 1998

ABSTRACT: Linear rheological properties of tightly-entangled isotropic solutions of semi-flexible polymers are calculated using a tube model, and qualitative predictions are given for the response of more dilute solutions. The linear complex modulus of a solution of long, tightly-entangled chains is dominated at low frequencies by a curvature contribution, analogous to the elastic stress of entangled flexible chains, that relaxes by reptation and gives rise to a broad elastic plateau. The modulus is dominated at higher frequencies by a larger tension contribution, whose frequency dependence is controlled at intermediate frequencies by the diffusion of excess length along the tube and at very high frequencies by the unhindered transverse motion of the chain within the tube. This high-frequency regime yields a complex modulus that varies as $G^*(\omega) \propto (i\omega)^{3/4}$ with frequency ω. Solutions of shorter, rod-like chains also exhibit a slowly-decaying orientational contribution analogous to the elastic stress found in solutions of true rigid rods. The linear response of the flow birefringence and the effect of cross-links between chains are also discussed.

I. Introduction

In the following, we use the primitive chain model and stress tensor introduced in the preceding article,[1] hereafter referred to as "(I)", to calculate the linear viscoelastic response and linear flow-birefringence of semidilute isotropic solutions of semiflexible chains. We focus here primarily on describing a regime of isotropic but "tightly-entangled" solutions in which each chain is confined to a tube of diameter D_e much less than its persistence length L_p.

The tube model used here to describe the tightly-entangled phase is defined physically by the following assumptions: (i) each polymer is confined over short times to a well-defined tube with $D_e \ll L_p$, (ii) each polymer may move relatively freely along the tube, hindered only by viscous dissipation in the surrounding solvent, (iii) the conformation of the tube deforms affinely in response to macroscopic deformation of the solution, and (iv) excluded-volume interactions between polymers may be neglected except insofar as they act (by preventing chains from crossing) to constrain each polymer to a tube. Because the tube has a nonzero diameter, small transverse undulations of the polymer within the tube are allowed, and the dynamics of these undulation modes controls the high-frequency response of the model. The results obtained below constitute an almost exact calculation of the linear response of this physical model over a wide frequency range, with the fewest possible mathematical simplifications. The ability or inability of the model to descibe experimental results should thus primarily depend upon the validity of these physical assumptions.

As discussed in (I), this tightly-entangled regime is expected to occur over a range of values of the concentration ρ (the concentration of contour length per unit volume) for which $\rho^{**} \ll \rho \ll \rho_{nem}$, where ρ^{**} is the crossover concentration above which both the tube diameter and entanglement length become less than L_p, and ρ_{nem} is the critical concentration above which a nematic liquid-crystalline phase begins to form. For coil-like chains, of contour length $L \gg L_p$, the ratio ρ_{nem}/ρ^{**} is predicted to be proportional to the ratio L_p/d of the persistence length to the steric diameter d of the chain. For more rod-like chains, of length $L \lesssim L_p$, the ratio ρ_{nem}/ρ^{**} becomes smaller but remains largest when L/d is largest. The approach used here is thus very likely the appropriate one for describing concentrated isotropic solutions of actin filaments,[2−24] for which $L_p/d \simeq 10^3$ and $L_p \sim L$, as is confirmed by the results of video microscopy that show the confinement of flourescently labeled actin filaments to a narrow tube.[19,20] The model is also intended to serve as a useful starting point in the description of concentrated isotropic solutions of somewhat less rigid semiflexible polymers such as PBLG and DNA, for which $L_p/d \sim 20-100$, a starting point that is naturally complementary to that taken in existing rigid-rod and related fuzzy-cylinder[25] models.

The plan of this paper is as follows: In section II, relatively simple arguments are used to construct a qualitative understanding of the physical mechanisms and time scales involved in the relaxation of stress and optical birefringence in solutions of wormlike chains. The discussion given here covers a somewhat broader range than that treated in the rest of the paper, since it includes qualitative discussions of the behavior expected in unentangled and loosely-entangled, as well as tightly-entangled, solutions. In sections III and IV, a more quantitative model is developed to describe the linear response of the stress (in section III) and flow birefringence (in section IV) of a tightly-entangled solution. Some technical details of this model have been organized into Appendices A−C, which discuss the following: (A) the equilibrium distribution of chain conformations, (B) the motion of a single tightly-entangled chain in a homogeneous flow field, and (C) the initial response of the stress to an infinitesimal step deformation. Section V is devoted to a comparison of the predicted viscoelastic response to that measured in recent experiments on *F*-actin solutions. Section VI contains concluding remarks.

S0024-9297(98)00304-0 CCC: $15.00
Published on Web 09/19/1998

II. Overview

To calculate the linear viscoelastic properties of a fluid, we estimate (in this section) or calculate (in section III) the relaxation of stress in a system that is subjected to an infinitesimal step strain $\delta\epsilon$ at time $t = 0$. The dynamic modulus $G(t)$ is defined by expressing the resulting stress $\boldsymbol{\sigma}(t)$ as a product

$$\boldsymbol{\sigma}(t) = G(t)(\delta\epsilon + \delta\epsilon^{\dagger}) \tag{1}$$

The complex modulus $G^*(\omega)$ is given by the Fourier transform

$$G^*(\omega) \equiv G'(\omega) + iG''(\omega) \tag{2}$$

$$\equiv i\omega\int_0^\infty \mathrm{d}t\ \mathrm{e}^{-i\omega t}\, G(t) \tag{3}$$

in which $G'(\omega)$ and $G''(\omega)$ are, respectively, the storage and loss moduli. The zero-frequency viscosity η_0 is given by the integral $\int_0^\infty \mathrm{d}t\ G(t)$.

In this paper, the stress $\boldsymbol{\sigma}$ will be approximated by the intramolecular stress $\boldsymbol{\sigma}_{\mathrm{intra}}$ that is given in eqs I.34−1.37 [occasional references to equations given in (I) will be denoted here by use of "I" as a prefix to the equation number; i.e. eqs I.34−I.37 are eqs 34−37 in (I)] as a sum

$$\boldsymbol{\sigma} = \boldsymbol{\sigma}_{\mathrm{curve}} + \boldsymbol{\sigma}_{\mathrm{orient}} + \boldsymbol{\sigma}_{\mathrm{tens}} - cT\boldsymbol{\delta} \tag{4}$$

where c is the number density of molecules. The physical origins of the curvature stress $\boldsymbol{\sigma}_{\mathrm{curve}}$, the orientational stress $\boldsymbol{\sigma}_{\mathrm{orient}}$, and the tension stress $\boldsymbol{\sigma}_{\mathrm{tens}}$ are discussed in (I). We neglect here the intermolecular stress $\boldsymbol{\sigma}_{\mathrm{inter}}$ calculated in section IV.B of (I), which arises from the excluded-volume interactions between molecules, which is expected to be small in most cases of interest here. The stress and moduli calculated below actually include only the polymeric stress contribution $\boldsymbol{\sigma}_{\mathrm{p}}$, as defined in eq I.22, and may be corrected to include the neglected bare solvent contribution by adding $\eta_s\delta(t)$ to our result for $G(t)$ or, equivalently, by adding $i\omega\eta_s$ to $G^*(\omega)$.

In section III, we give separate calculations of the relaxation of the stress components $\boldsymbol{\sigma}_{\mathrm{curve}}(t)$, $\boldsymbol{\sigma}_{\mathrm{orient}}(t)$, and $\boldsymbol{\sigma}_{\mathrm{tens}}(t)$, which all exhibit different characteristic relaxation times. We thus express $G(t)$, $G^*(\omega)$, and η_0 in what follows as sums of contributions arising from these three stress contributions, writing, for example,

$$G(t) = G_{\mathrm{curve}}(t) + G_{\mathrm{orient}}(t) + G_{\mathrm{tens}}(t) \tag{5}$$

where $\boldsymbol{\sigma}_{\mathrm{curve}}(t) = G_{\mathrm{curve}}(t)(\delta\epsilon + \delta\epsilon^{\dagger})$, etc., and similarly expanding $G^*(\omega)$ and η_0.

In section IV, we consider the linear response of the optical refractive index tensor $\mathbf{n}(t)$ to an imposed flow. The intrinsic polymeric contribution to the traceless component of $\mathbf{n}(t)$, which is expected to dominate the total birefringence in the concentration regimes of interest, is given by a tensor

$$\mathbf{n}(t) = \rho A\int_0^L \frac{\mathrm{d}s}{L}\left\langle \mathbf{u}(s)\,\mathbf{u}(s) - \frac{1}{3}\boldsymbol{\delta}\right\rangle \tag{6}$$

in which A is a material constant proportional to the anisotropy of the polarizability per unit length of polymer. The linear response of $\mathbf{n}(t)$ following an infinitesimal step deformation is described by a function $\mu(t)$, such that

$$\delta\mathbf{n}(t) = \mu(t)(\delta\epsilon + \delta\epsilon^{\dagger}) \tag{7}$$

and a corresponding frequency-dependent response function

$$\mu^*(\omega) \equiv \mu'(\omega) + i\mu''(\omega) \tag{8}$$

where $\mu^*(\omega) \equiv i\omega\int_0^\infty \mathrm{d}t\ \mathrm{e}^{-i\omega t}\,\mu(t)$.

Table 1. Characteristic Modulus and Time Scales

Moduli	
$G_{\mathrm{orient}} \sim \rho T/L$; $G_{\mathrm{curve}} \sim \rho T/L_e$; $G_{\mathrm{tens}} \sim \rho T L_p^2/L_e^3$	
Time Scales	
$\tau_{\mathrm{rep}} \propto L^3$	disengage by reptation
$\tau_{\mathrm{end}} \propto L L_p^3$	randomize end orientation, $L \gg L_p$
$\tau_{\mathrm{rod}} \propto L L_p^2$	randomize rod orientation, $L \ll L_p$
$\tau_{\phi p} \propto L_e^3$	transport ϕ by L_p, $L \gg L_p$
$\tau_{\phi L} \propto L_e^3 L^2/L_p^2$	transport ϕ by L, $L \gg [L_p L_e]^{1/2}$
$\tau_{\|} \propto L^8/L_p^5$	transport ϕ by L, $L \ll [L_p L_e]^{1/2}$
$\tau_e \propto L_e^4/L_p$	undulation, wavelength L_e
$\tau_p \propto L_p^3$	undulation, wavelength L_p, $L \gg L_p$
$\tau_L \propto L^4/L_p$	undulation, wavelength L, $L \ll L_p$
$\tau_c \propto L_p^3(L/L_p)^{\alpha}$	Rouse−Zimm time, $L \gg L_p$

[a] The last three times scales listed are those relevant to dilute solutions.

A. Time Scales. We now identify a set of time scales relevant to viscoelastic behavior, by considering the characteristic time scales for the decay of $G_{\mathrm{curve}}(t)$, $G_{\mathrm{orient}}(t)$, and $G_{\mathrm{tens}}(t)$. These relaxation times are identified here by simple physical arguments similar in spirit to those used previously by Isambert and Maggs.[26,27] Many of the definitions given below do, however, contain numerical prefactors that are chosen so as to simplify the presentation of quantitative results in sections III and IV. A summary of relaxation times, and of characteristic free energy scales for the moduli, is given in Table 1.

To describe the motion of a single chain, we introduce two friction coefficients, ζ and $\zeta_\perp$, which give the frictional force per unit chain length and per unit velocity of the chain relative to the surrounding matrix of chains, where ζ is a coefficient for motion of the chain parallel to its own contour and $\zeta_\perp$ is a coefficient for transverse undulations of the polymer within the tube. These friction coefficients may be estimated by simple hydrodynamic arguments,[29,30,31,32] which yield values

$$\zeta \simeq \frac{2\pi\eta_s}{\ln(\xi/d)} \tag{9}$$

$$\zeta_\perp \simeq \frac{4\pi\eta_s}{\ln(\xi_\perp/d)} \tag{10}$$

in which η_s is the solvent viscosity and ξ and $\xi_\perp$ are hydrodynamic screening lengths describing the distance to which the fluid velocity field created by a moving polymer penetrates away from the polymer backbone. In numerical calculations, we will approximate both ξ and $\xi_\perp$ by the mesh size $\rho^{-1/2}$.

(1) Reptation. The curvature and orientation stress both relax as a result of reptation, i.e., as a result of the Brownian motion of the polymer along its own contour.[33] This curvilinear diffusion is characterized by

a diffusivity given by the Einstein relation

$$D_{rep} = T/(\zeta L) \tag{11}$$

where the friction coefficient ζ is independent of L.

The contribution of a chain segment to the curvature stress relaxes immediately when the segment is carried by diffusion to the end of the primitive chain, when it is destroyed and replaced by a segment whose curvature (but not its orientation) is chosen randomly from an equilibrium probability distribution. We showed in (I) that the contribution of a segment of chain to the curvature stress vanishes as soon as the curvature within that segment is equilibrated. As a result, the longest relaxation time for the curvature stress is given by the disengagement time

$$\tau_{rep} \equiv L^2/\pi^2 D_{rep} \propto L^3 \tag{12}$$

which is on the order of the time needed for the polymer to diffuse its own contour length.

The orientational stress relaxes with a relaxation time given by the time required to randomize the orientation of the ends of the chain. This criterion follows from the definition of $\boldsymbol{\sigma}_{orient}$ in eq I.36, where $\boldsymbol{\sigma}_{orient}$ is defined so as to depend only upon the orientation of the chain ends. In the limit of coil-like chains, with $L \gg L_p$, the polymer must diffuse only a distance of order L_p to randomize the orientation of the end, giving a relaxation time

$$\tau_{end} \equiv {L_p}^2/D_{rep} \propto L{L_p}^2 \tag{13}$$

which in this limit is much less than τ_{rep}.[28] In the limit of rod-like polymers, with $L \ll L_p$ the relaxation of the orientation of the polymer (which in this limit rotates as an almost rigid body) is found in refs 34−36 and in section III of this paper to occur with a relaxation time

$$\tau_{rod} \equiv LL_p/6D_{rep} \propto L^2 L_p \tag{14}$$

This time is much longer than τ_{rep}, reflecting the fact that in this regime the chain must diffuse many times its own length before its overall orientation is randomized.

Equation 14 for τ_{rod} may be understood qualitatively as follows:[34] Rotational diffusion in the tightly-entangled regime may be described as a series of random steps, each involving disengagement of the polymer from the tube, which occur with an average time step $\Delta t \sim \tau_{rep} \propto L^2/D_{rep}$. Each such step results in the formation of a new tube, with an end-to-end orientation that differs from the orientation of the previous tube by a typical angular deviation $\Delta\theta \propto \Delta h/L$, where $\Delta h \propto L^{3/2}/{L_p}^{1/2}$ is the root mean square transverse fluctuation of a chain segment of length L in thermal equilibrium. This yields a rotational diffusivity of order $D_{rod} \propto (\Delta\theta)^2/\Delta t \propto D_{rep}/(LL_p)$, and thus a time $\tau_{rod} \propto LL_p/D_{rep}$ to diffuse an angle of order unity.

(2) Contour Density Fluctuations. A nonzero value of the tension stress $\boldsymbol{\sigma}_{tens}$ is produced when segments of the primitive chain are stretched or compressed tangentially. Though the polymer contour is assumed to be inextensible, the primitive (or coarse-grained) chain can accommodate a small amount of extension or compression by locally suppressing or enhancing the extent of the "wrinkling" of the polymer within the tube. To describe this, we introduce a dimensionless contour length density $\phi(s,t)$ which is defined as the length of polymer contour length per unit length of the primitive chain or tube, averaged over a segment of tube of length L_e. The density ϕ is always slightly greater than 1 as a result of the wrinkling of the polymer with the tube. It may be expressed in terms of the variables of the primitive chain models as a ratio $\phi(s) \equiv L_e/q(s)$ and approaches a value $\phi_{eq} \equiv L_e/a$ in thermal equilibrium. To calculate the linear response of the solution, we may use a linear approximation for the tension as

$$\mathcal{T}(s) \simeq -B\,(\phi(s) - \phi_{eq})/\phi_{eq} \tag{15}$$

where B is the effective extension modulus for a chain segment of length L_e. This modulus was estimated by MacKintosh et al.,[37] whose result is reproduced in eq I.20.

The fractional extension of a chain segment with orientation $\mathbf{u}(s)$ within a solution subjected to a infinitesimal affine step deformation by a strain $\delta\epsilon$ is given by $\delta\epsilon$:$\mathbf{uu}$, and so

$$\phi(s) \simeq \phi_{eq} - \phi_{eq}\delta\epsilon{:}\mathbf{u}(s)\,\mathbf{u}(s) \tag{16}$$

is the initial value of $\phi(s)$ immediately after such a deformation, which depends upon the local chain orientation $\mathbf{u}(s)$.

The relaxation of $\phi(s)$ to its equilibrium value after a step deformation occurs by tangential motion of the chain along the tube, which, we now show, may be described as a diffusive process. The temporal evolution of $\phi(s,t)$ on a specified polymer may be described (after the cessation of macroscopic flow) by a continuity equation

$$\frac{\partial\phi}{\partial t} = -\frac{\partial}{\partial s}(\bar{v}\phi) \tag{17}$$

in which $\bar{v}(s)$ is the tangential velocity of the polymer relative to the tube. The tangential velocity $\bar{v}$ is driven by gradients in the tension and so is related to $\mathcal{T}(s)$ by a force balance equation

$$\zeta\bar{v}(s) = \frac{\partial\mathcal{T}(s)}{\partial s} \tag{18}$$

in which $\zeta\bar{v}(s)$ is the frictional force per unit length exerted upon the chain as it is dragged along the tube. By substituting approximation eq 15 for $\mathcal{T}(s)$ into eq 18, and the resulting expression for $\bar{v}(s)$ into eq 17, one obtains a diffusion equation

$$\frac{\partial\phi}{\partial t} \simeq D_\phi \frac{\partial^2\phi}{\partial s^2} \tag{19}$$

in which

$$D_\phi \equiv \frac{B}{\zeta} \propto \frac{T}{\zeta}\frac{{L_p}^2}{{L_e}^3} \tag{20}$$

is a diffusivity for contour length density.[38]

Because the initial value of $\phi(s)$ given in eq 16 depends upon the local chain orientation, the initial values of $\phi(s)$ at two points s and s' on the same chain will remain correlated over separations $|s - s'| \sim L_p$ for

chains of length $L \gg L_p$ and over the entire chain length for chains of length $L \ll L_p$. The time needed for tension to relax to a small fraction of its initial value is thus given in the limit $L \gg L_p$ of coil-like chains by the time

$$\tau_{\phi p} \equiv L_p^2/9D_\phi \propto L_e^3 \tag{21}$$

needed for excess length to diffuse a distance of order L_p, and in the rod-like limit $L \ll L_p$ by the time

$$\tau_{\phi L} \equiv L^2/\pi^2 D_\phi \propto L_e^3 L^2/L_p^2 \tag{22}$$

needed for excess length to diffuse the full chain length. These relaxation times are expected to vary as

$$\tau_{\phi L} \propto \zeta L^2/B \propto \rho^{-6/5} L_p^{-7/5} L^2 \tag{23}$$

$$\tau_{\phi p} \propto \zeta L_p^2/B \propto \rho^{-6/5} L_p^{3/5} \tag{24}$$

with changes in the parameters ρ, L, and L_p. It is important to note that these relaxation times are inversely proportional to B, while the tension modulus G_{tens} is proportional to B, so that the formation of a large tension modulus automatically yields short relaxation times.

Our discussion has thus far been based upon the primitive chain model introduced in (I), which is intended only to describe behavior at time scales longer than an entanglement time

$$\tau_e \sim \zeta_\perp L_e^4/TL_p \tag{25}$$

which is the relaxation time of an undulation mode of wavelength L_e.

Our discussion has thus far also implicitly assumed that the relaxation times $\tau_{\phi L}$ and $\tau_{\phi p}$ remain longer than τ_e, since our calculation of $\tau_{\phi L}$ and $\tau_{\phi p}$ made use of an extension modulus B that was calculated (in Appendix B of I) by assuming that all modes of wavelength less than L_e were effectively equilibrated at these times. Upon comparing $\tau_{\phi L}$ and $\tau_{\phi p}$ to τ_e, we find that this is a consistent assumption for all chains of length $L \gtrsim [L_p L_e]^{1/2}$ (and thus for all chains of length $L \gtrsim L_p$) but becomes inconsistent for rod-like chains of length $L \lesssim [L_p L_e]^{1/2}$, for which eqs 21 and 25 yield $\tau_{\phi L} \lesssim \tau_e$.

The relaxation time for tension in these very short chains with $L \lesssim [L_p L_e]^{1/2}$ is instead given roughly by the time

$$\tau_{||} = L^2/D_\phi(\tau_{||}) \tag{26}$$

required for tension to diffuse the length of the chain, as calculated self-consistently using a time-dependent diffusion constant $D_\phi(t) \equiv B(t)/\zeta$ and extension modulus $B(t)$ evaluated at a time $t \sim \tau_{||}$. Using the approximation of eq I.60 for $B(t)$, which yields $B(t) \propto t^{-3/4}$ for $t \ll \tau_e$, and solving for $\tau_{||}$ yields a time

$$\tau_{||} \sim \zeta L^8/TL_p^5 \tag{27}$$

that quickly becomes much less than τ_e. For rods of length $L \lesssim [L_e L_p]^{1/2}$, the tension can thus relax via tangential motion even before entanglement begins to hinder the relaxation of undulation modes.

(3) Unentangled Chains. To describe unentangled and loosely-entangled chains, we also introduce time scales

$$\tau_p \sim \zeta_\perp L_p^3/T \tag{28}$$

$$\tau_L \sim \zeta_\perp L^4/TL_p \tag{29}$$

that give, respectively, the relaxation time for a bending mode of contour wavelength approaching L_p on a coil-like chain, of length $L \gg L_p$, and the relaxation time for the longest wavelength bending mode of a rod-like chain, of length $L \ll L_p$.

In the case of unentangled coil-like chains, modes of contour wavelength much longer than L_p are best described as modes of a course-grained Rouse or Zimm model of a flexible chain, in which the relaxation frequency of a mode of contour wavenumber q is found to vary with q as $\omega(q) \propto \tau_p^{-1}(qL_p)^\alpha$ for $L_p < q^{-1} < L$, where $\alpha = 2$ for free-draining (Rouse) Gaussian chains, $\alpha = {}^3/_2$ for hydrodynamically interacting (Zimm) Gaussian chains, and $\alpha \simeq 1.8$ for hydrodynamically interacting self-avoiding chains.[39] Such unentangled coil-like chains exhibit a terminal relaxation time

$$\tau_c \sim \tau_p(L/L_p)^\alpha \tag{30}$$

given by the relaxation time for a mode with $q \sim 1/L$.

B. Viscoelastic Response. We now combine the above discussion of time scales with our discussion of the free energy scales of the different stress contributions in (I) to obtain a qualitative description of the frequency dependence $G^*(\omega)$ in various regimes of concentration and chain length. The characteristic free energy scales for the three instantaneous moduli $G_{curve}(0)$, $G_{tens}(0)$, and $G_{orient}(0)$ of the primitive chain model (which will appear in $G^*(\omega)$ as plateau moduli) are given in eqs I.42 and I.43 and form a hierarchy

$$G_{tens}(0) \gg G_{curve}(0) \gg G_{orient}(0) \tag{31}$$

In what follows, we will discuss separately the limits of coil-like and rod-like chains. In each case we will first discuss the behavior predicted in the tightly-entangled regime and then make comparisons to the behavior expected for loosely-entangled and unentangled solutions.

(1) Coil-like Chains: $L \gg L_p$. In the limit of coil-like chains, the decay times for the three stress contributions form a hierarchy

$$\tau_{rep} \gg \tau_{end} \gg \tau_{\phi p} \tag{32}$$

Because $G_{orient}(t)$ is seen to decay with a time τ_{end} much smaller than the decay time τ_{rep} for $G_{curve}(t)$, while also having an initial value $G_{orient}(0) \ll G_{curve}(0)$, the orientational contribution is expected to make a negligible contribution to $G(t)$ at all times, and thus may be ignored in this limit. The total modulus $G(t)$ may thus be approximated here as the sum of a large but rapidly decaying tension contribution $G_{tens}(t)$ and a much smaller but more slowly decaying curvature contribution $G_{curve}(t)$, as pointed out previously by Maggs.[27] If the time scales τ_{rep}, $\tau_{\phi p}$, and τ_e become sufficiently widely separated, this will lead to a complex modulus $G^*(\omega)$ of the form shown in Figure 1, which can in principle exhibit two distinct plateaus: a low-frequency, curvature-dominated plateau within which $G'(\omega) \simeq G_{curve}(0)$ and

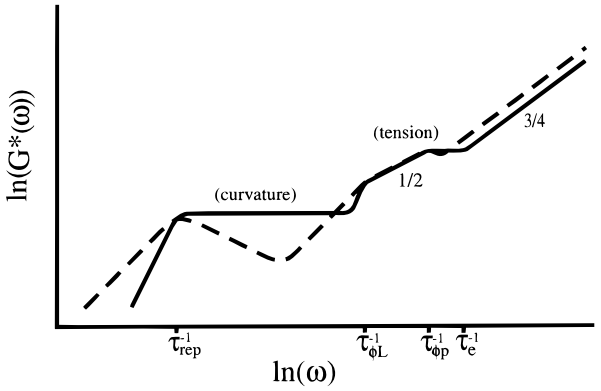

Figure 1. Schematic of $G'(\omega)$ (solid line) and $G''(\omega)$ (dotted line) for a tightly-entangled solution of coil-like chains, with $L \gg L_p$, as suggested by arguments given in section II. Slopes indicate regimes with a nontrivial power law dependence on frequency, and (curvature) and (tension) indicate frequency regimes in which $G^*(\omega)$ is dominated by curvature or tension contributions. Time scales are defined in the text.

a higher-frequency tension-dominated plateau within which $G'(\omega) \simeq G_{tens}(0)$.

The curvature stress, which dominates the low-frequency plateau, has a free energy scale of order T per entanglement and is predicted to vary with ρ, L, and L_p as

$$G_{curve}(0) \propto \rho T/L_e \propto \rho^{7/5} L_p^{-1/5} \tag{33}$$

where we have taken $L_e \sim L_p(\rho L_p^2)^{-2/5}$, as in eq I.5.

The tension stress, which dominates the high-frequency behavior of $G^*(\omega)$, exhibits a more complex frequency dependence:

For frequencies $\omega \lesssim \tau_e^{-1}$, the tension stress may be calculated within the context of the primitive chain model. For chains of length $L \gg L_p$, this model is found to lead to a plateau in $G'(\omega)$ that extends over frequencies $\tau_{\phi p}^{-1} \lesssim \omega \lesssim \tau_e^{-1}$, with a predicted plateau value

$$G_{tens}(0) \propto \rho B \propto T\rho^{11/5} L_p^{7/5} \tag{34}$$

where we have taken $B \sim TL_p^2/L_e^3$, as in eq I.20. This plateau modulus, which is larger than $G_{curve}(0)$ by a factor of order $(L_p/L_e)^2$, is the one predicted by MacKintosh et al.,[37] who focused exclusively on this contribution to the stress but did not allow for any relaxation of the tension. We find in section IV that, for $L \gg L_p$, $G^*_{tens}(\omega)$ varies with frequency as $G^*_{tens}(\omega) \propto (i\omega)^{1/2}$ for frequencies $\tau_{\phi L}^{-1} \ll \omega \ll \tau_{\phi p}^{-1}$ and exhibits fluidlike terminal behavior with $G^*(\omega) \propto i\omega$ at frequencies $\omega \lesssim \tau_{\phi L}^{-1}$.

At frequencies $\omega \gg \tau_e^{-1}$, $G^*_{tens}(\omega)$ may no longer be calculated using the primitive chain model, which assumes equilibration of the polymer within the tube. We argued in (I) that the behavior of $G^*_{tens}(\omega)$ in this high-frequency regime could be predicted by assuming that when the solution is subjected to an oscillatory deformation with frequency ω, only those short-wavelength undulation modes whose decay times are shorter than ω^{-1} can provide a reservoir of excess length and thereby contribute to the effective extensibility of the chain. In section IV, we make this notion more precise by first expressing $G_{tens}(\omega)$ in terms of a frequency-dependent extension modulus $\hat{B}(\omega)$ that describes the response of $\phi(s,t)$ to a sinusoidally oscillating tension

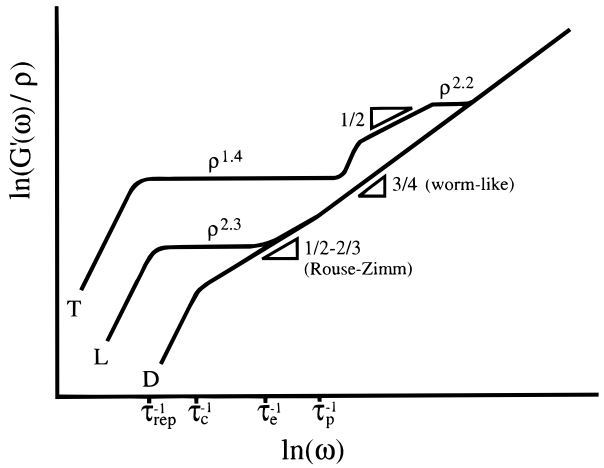

Figure 2. Schematic of evolution of $G'(\omega)/\rho$ with ρ for solutions of coil-like chains. The three lines are sketches of behavior predicted for dilute or unentangled solutions (D), loosely-entangled solutions (L), and tightly-entangled solutions (T), all of which exhibit a common asymptote for $G^*(\omega)/\rho$ at high frequencies. Slopes represent regimes with a nontrivial power law dependence on frequency, and powers of ρ indicate the predicted dependence of the plateau moduli on concentration. Time scales shown are those relevant to the dilute and loosely-entangled regime, so τ_{rep} is the reptation time of the loosely-entangled solution.

$\mathcal{T}(s,t)$, and then calculating $\hat{B}(\omega)$ by considering the dynamics of transverse fluctuations of the polymer within the tube. We thereby obtain a universal high-frequency limiting form for the complex modulus as

$$\lim_{\omega \gg \tau_e^{-1}} G^*_{tens}(\omega) \simeq \frac{2^{3/4}}{15} \frac{\rho T}{L_p} \left(i\omega \frac{\zeta_\perp L_p^3}{T} \right)^{3/4} \tag{35}$$

which is of the form obtained in (I) by scaling arguments but which now contains a precise numerical prefactor.

We now consider briefly the behavior of unentangled and loosely-entangled coils and the evolution of $G^*(\omega)$ with increasing concentration. In Figure 2, we sketch the expected frequency dependence of the ratio $G'(\omega)/\rho$ (because this ratio approaches a concentration-independent limiting form at high frequencies) in each concentration regime.

Dilute solutions of coils, with concentrations below the overlap concentration ρ^*, are expected to exhibit three frequency regimes: For all $\omega \gg \tau_p^{-1}$, $G^*(\omega)$ is expected to exhibit the high-frequency limiting behavior of eq 35. For all $\omega \ll \tau_p^{-1}$, the frequency dependence of $G^*(\omega)$ is describable by a Rouse or Zimm model, with eigenfrequencies $\omega \propto q^\alpha$. These models yield complex moduli of the form

$$G^*(\omega) \sim \frac{\rho T}{L_p} (i\omega\tau_p)^{1/\alpha} \tag{36}$$

with $^1/_2 \le \alpha^{-1} \le {}^2/_3$, over the frequency range $\tau_c^{-1} \ll \omega \ll \tau_p^{-1}$ in which $G^*(\omega)$ is dominated by modes of wavelengths between L_p and L, and yield fluidlike terminal behavior, with $G^*(\omega) \propto i\omega$, for $\omega \ll \tau_c^{-1}$.

Loosely-entangled solutions of semiflexible coils, with concentrations $\rho^* \ll \rho \ll \rho^{**}$, are (by definition) characterized by an entanglement length $L_e \gg L_p$, and exhibit viscoelastic behavior identical to that of entangled solutions of flexible chains for all $\omega \ll \tau_p^{-1}$. In this regime, $G'(\omega)$ develops an elastic plateau with a plateau modulus $G' \sim \rho T/L_e$ that extends over a

frequency range $\tau_{rep}^{-1} \ll \omega \ll \tau_e^{-1}$. We use τ_{rep} here to refer to the disengagement time of a loosely-entangled chain and τ_e to refer to the Rouse−Zimm relaxation time of a flexible subchain of contour length L_e, with $L_e \gg L_p$. In studies of entangled solutions of flexible polymers, the plateau modulus has been found experimentally to vary with ρ roughly as $G' \propto \rho^{2.3}$, both in good solvents[40] and in Θ-solvents.[41,42] The disengagement time τ_{rep} is also found to increase with increasing concentration in this regime, because the contour length of the primitive chain increases as the tube diameter falls, but is expected to stop increasing with increasing ρ in the tightly-entangled regime, in which the contour length of the primitive chain becomes nearly equal to the true chain length. At frequencies $\omega \gg \tau_e^{-1}$, the behavior of $G^*(\omega)/\rho$ is expected to become identical to that of a dilute solution, giving $G^*(\omega) \propto (i\omega)^{1/\alpha}$ for frequencies $\tau_e^{-1} \ll \omega \ll \tau_p^{-1}$ and $G^*(\omega) \propto (i\omega)^{3/4}$ for frequencies $\omega \gg \tau_p^{-1}$.

Upon entering the tightly-entangled regime, one thus expects to see the following: (i) the disappearance of the remaining Rouse−Zimm regime in which $G^*(\omega) \propto (i\omega)^{1/\alpha}$; (ii) a change in the ρ-dependence of the plateau modulus from $G' \propto \rho^{2.3}$ for $\rho \ll \rho^{**}$ to $G' \propto \rho^{1.4}$ for $\rho \gg \rho^{**}$; (iii) a saturation in the value of τ_{rep} with increasing concentration; (iv) the development at sufficiently high concentrations of a second, tension-dominated plateau at frequencies $\omega \gtrsim \tau_{\phi p}^{-1}$. The predicted width of the tension-dominated plateau vanishes for $\rho \sim \rho^{**}$, so this feature is found in numerical calculations to first appear as a slight shoulder in $G'(\omega)$ and to then widen only slowly with increasing ρ.

In subsection III.C, we present results of numerical calculations of $G^*(\omega)$, calculated using the a tube model of tightly-entangled solutions, for solution with parameters roughly appropriate to a 1 mg/mL solution of *F*-actin. The results are generally similar to those predicted above on the basis of qualitative arguments, except for the notable absence of any tension-dominated plateau. The fact that the model does not yield a tension-dominated plateau for parameters typical of actin solutions, in which $L_p/d \sim 10^3$ and $\rho L_p^2 \sim 10^4$, suggests that while the appearance of such a plateau is a theoretical possibility, it may in practice be impossible to find a model system for which the parameter ρL_p^2 is large enough to produce a well-defined second plateau.

This last conclusion relies critically, however, upon our assumption that the motion of the polymers along the tube is resisted only by viscous dissipation in the solvent. The presence of even a small density of cross-links between chains, or any other impediment to tangential motion, could produce a tension-dominated plateau with a large plateau modulus extending to low frequencies and thus drastically alter our results.

(2) Rod-like Chains: $L \ll L_p$. The most obvious difference between the rod-like and coil-like regimes is that, in the rod-like regime, the time τ_{rod} for the relaxation of $G_{orient}(t)$ is longer than the time τ_{rep} for the relaxation of $G_{curve}(t)$, so that the orientational contribution can make a signficant contribution to the low-frequency behavior of $G^*(\omega)$.

The time dependence of $G_{orient}(t)$ in a solution of rod-like polymers is controlled by the decay of anisotropies in the distribution of chain orientations. This decay can be described in any of the three isotropic concentration regimes as a diffusive process and results in all three regimes in an exponential dependence on time, of the form

$$G_{orient}(t) = \frac{3}{5}\frac{\rho T}{L} e^{-t/\tau_{rod}} \tag{37}$$

Here, the prefactor is a measure of the free energy cost for aligning a set of noninteracting rods by deforming the surrounding fluid, and τ_{rod} is the time needed to rerandomize the rod orientations. In the dilute regime, τ_{rod} becomes independent of concentration and varies with L roughly as $\tau_{rod} \simeq \zeta L^3/T$, to within logarithmic corrections arising from hydrodynamic self-interactions.[43] In the loosely-entangled regime, τ_{rod} has been predicted to increase with increasing concentration as $\tau_{rod} \simeq (\zeta L^3/T)(\rho L^2)^\gamma$, where $\gamma = 2$ in the DE cage model of semidilute rigid rods[44] and $\gamma = 1$ in a competing model introduced by Fixman.[45,46] In the tightly-entangled regime, τ_{rod} is given by eq 14, which yields a value that is independent of ρ but that depends upon L_p.

In discussing the frequency dependence of the curvature and tension moduli, it is useful to distinguish two cases, depending on the relative magnitudes of the lengths L and $[L_p L_e]^{1/2}$:

For chains of length $L \ll [L L_p]^{1/2}$, the tension can relax via diffusion to the ends of the chain with a relaxation time $\tau_{||}$ less than the entanglement time τ_e, so the relaxation times form a hierarchy

$$\tau_{rod} \gg \tau_{rep} \gg \tau_e \gg \tau_{||} \tag{38}$$

In this regime, $G'_{tens}(\omega)$ is not expected to ever exhibit a high-frequency tension-dominated plateau and instead exhibits a low-frequency orientation-dominated plateau for $\omega \gtrsim \tau_{rod}^{-1}$, a curvature-dominated plateau for $\omega \gtrsim \tau_{rep}^{-1}$, and a tension-dominated power law regime in which $G^*(\omega) \propto (i\omega)^{3/4}$ for $\omega \gtrsim \tau_{||}^{-1}$, as shown in Figure 3. In this regime, the low-frequency behavior of $G^*(\omega)$ is dominated by $G_{orient}(\omega)$.

For chains of length $L_p \gg L \gg [L_p L_e]^{1/2}$, the time $\tau_{\phi L}$ for relaxation of tension becomes larger than τ_e, and so we obtain a hierarchy of time scales

$$\tau_{rod} \gg \tau_{rep} \gg \tau_{\phi L} \gg \tau_e \tag{39}$$

similar to that found for coil-like chains, except for the appearance of τ_{rod} as the longest relaxation time. As for coil-like chains, $G'(\omega)$ may thus in principle exhibit both a lower-frequency curvature-dominated plateau and a higher-frequency tension-dominated plateau. The curvature modulus is easily shown to become large enough to dominate the low-frequency limit of $G''(\omega)$ (and thus dominate η_0) for all $L \gtrsim L_p^{1/2} L_e^{1/2}$ and to dominate the low-frequency limit of $G'(\omega)$ (and thus destroy the orientation-dominated plateau in $G'(\omega)$) for all $L \gtrsim L_p^{2/3} L_e^{1/3}$.

We now consider the behavior of unentangled and loosely-entangled solutions. The only qualitative difference between unentangled and loosely-entangled solutions of rods is the difference in the value of the orientational relaxation time τ_{rod}, which in a loosely-entangled solution is predicted to vary with concentration and to interpolate between the concentration-independent values of $\tau_{rod} \sim \zeta L^3/T$ characteristic of a dilute solution and $\tau_{rod} \sim \zeta L^2 L_p/T$ predicted for a tightly-entangled solution.

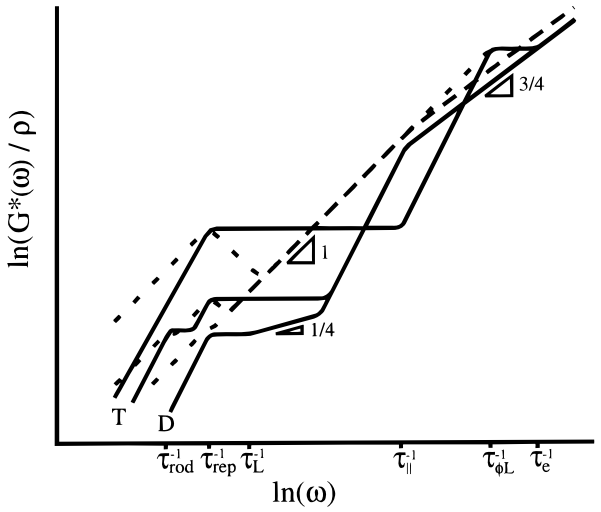

Figure 3. Schematic of the predicted evolution of $G'(\omega)/\rho$ (solid lines) and $G''(\omega)/\rho$ (dotted lines) with concentration for a solution of semiflexible rod-like polymers. Of the three concentrations shown, one is in the dilute regime (D) and two in the tightly-entangled regime (T), one for $L > L_p^{2/3}L_e^{1/3}$ (which exhibits a high-frequency tension-dominated plateau but no low-frequency orientation-dominated plateau) and one for $L < L_p^{1/2}L_p^{1/2}$ (which exhibits no tension-dominated plateau but exhibits a narrow orientation-dominated plateau and a low-shear viscosity with a signficant orientational contribution.) The time τ_{rod}^{-1} refers to the orientational relaxation time of the tightly-entangled solution. The corresponding relaxation time for the dilute solution is of order τ_{rep}, as shown. A loosely-entangled solution (not shown) would look similar to the dilute solution except for the appearance of a value of τ_{rod}^{-1} intermediate between those of dilute and tightly-entangled solutions. The overlapping lines for $G''(\omega)/\rho$ at intermediate frequencies, between τ_{rep}^{-1} and $\tau_{||}^{-1}$, where $G''(\omega) \propto \omega$, all correspond to the behavior obtained for the viscous (i.e., tension) contribution to the polymer stress of a solution of rigid rods.

The curvature modulus $G^*_{curve}(\omega)$ in an unentangled or loosely-entangled solutions is predicted in (I) to exhibit a power law behavior

$$G^*_{curve}(\omega) \propto \frac{\rho T}{L_p}\left(i\omega\frac{\zeta_\perp L_p^{\,3}}{T}\right)^{1/4} \qquad (40)$$

for all $\omega \gtrsim \tau_L^{-1}$, and is expected to exhibit fluidlike behavior for $\omega \lesssim \tau_L^{-1}$. This contribution becomes greater than $G^*_{orient}(\omega)$ for all $\omega \gtrsim \tau_L^{-1}$, leading to a curvature-dominated power law regime in which $G^*(\omega) \propto (i\omega)^{1/4}$, as shown in Figure 3.

The tension contribution to $G^*(\omega)$ in an unentangled or loosely-entangled solution of rods is expected to exhibit the limiting behavior of eq 35 for all $\omega \gg \tau_{||}^{-1}$ and to exhibit fluidlike behavior for $\omega \ll \tau_{||}^{-1}$.

Upon entering the tightly-entangled regime, by increasing either the concentration or chain length of a solution of semiflexible rods, one thus expects to see the following: (i) the orientational relaxation time τ_{rod} become almost concentration independent; (ii) the curvature-dominated power law regime predicted for loosely-entangled chains, in which $G^*(\omega) \propto (i\omega)^{1/4}$, evolve into a curvature-dominated plateau, with a plateau modulus $G' \propto \rho^{1.4}$; (iii) at higher concentrations or chain lengths, for which $L \gtrsim [L_pL_e]^{1/2}$, the curvature stress begin to dominate η_0 and a high-frequency tension-dominated plateau begin to form at frequencies $\tau_{\phi L}^{-1} \lesssim \omega \lesssim \tau_e^{-1}$; (iv) for $L \gtrsim L_p^{2/3}L_e^{1/2}$, the disappearance of any orientation-dominated plateau in $G'(\omega)$, as a result of the growth of $G'_{curve}(\omega)$. For the largest concentrations and/or chain lengths discussed above, the frequency dependence thus becomes rather similar to that predicted for coil-like chains, the only qualitative difference being the absence in solutions of rod-like chains of a power law regime in which $G^*_{tens}(\omega) \propto (i\omega)^{1/2}$, which is predicted to appear only for $L \gg L_p$.

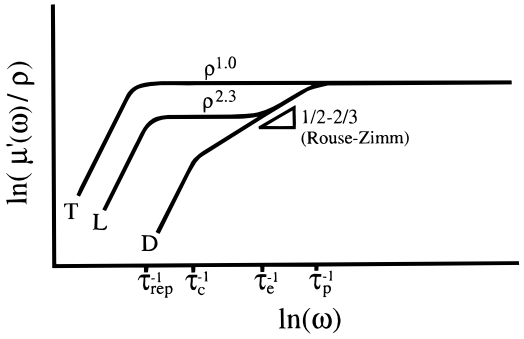

Figure 4. Schematic of the evolution of flow-birefringence response function $\mu'(\omega)$ with ρ, for solutions of coil-like chains, with the same notation as in Figure 2.

C. Optical Response. In section V, we consider the linear response of the intrinsic optical refractive index, which we describe by the response function $\mu(t)$ defined in eq 7. The intrinsic refractive index is sensitive only to the alignment of chain segments and not to the more rapid relaxation of tension. As a result, $\mu(t)$ is generally found to exhibit a simpler time dependence than $G(t)$.

The initial effect of a small step deformation, in any concentration regime is to rotate each chain segment by an amount proportional to the strain, producing an initial value

$$\lim_{t\to 0} \mu(t) \propto A\rho \qquad (41)$$

that is directly proportional to the concentration, where A is a material parameter, with similar prefactors in different concentration regimes.

The expected frequency dependence of the function $\mu'(\omega)$ for a system of coil-like chains, with $L \gg L_p$, is shown schematically in Figure 4 for the cases of tightly-entangled, loosely-entangled, and unentangled chains. In the tightly-entangled regime, the anisotropy produced by a step deformation can relax only via reptation, since the rapid relaxation of tension that complicates stress relaxation in this regime has no effect upon the distribution of segment orientations. In this regime, $\mu(t)$ is thus found to relax almost exponentially with a relaxation time τ_{rep}, as in the DE model, leading to a single plateau in $\mu'(\omega)$ for all $\omega \gtrsim \tau_{rep}^{-1}$.

In the loosely-entangled and unentangled regimes, $\mu(t)$ remains nearly constant up to a time of order τ_p but may then begin to relax via the relaxation of Rouse−Zimm modes with wavelengths greater than L_p. The relaxation of $\mu(t)$ at times $t \gg \tau_p$ may thus be described by Rouse−Zimm models designed to describe flexible chains, giving a stress−optic relation

$$\lim_{t\gg\tau_p} \mu(t) \simeq \frac{AL_p}{T}\, G(t) \qquad (42)$$

at these times. Correspondingly, the function $\mu^*(\omega)$ is expected to mimic the frequency dependence of $G^*(\omega)$ at all frequencies $\omega \lesssim \tau_p^{-1}$, which in a loosely-entangled solution leads to a low-frequency plateau in $\mu'(\omega)$ for

$\tau_{rep}^{-1} \lesssim \omega \lesssim \tau_e^{-1}$, in addition to the high-frequency plateau expected for all $\omega \gtrsim \tau_p^{-1}$.

In the limit of rod-like chains, with $L \ll L_p$, the refractive index $\mathbf{n}(t)$ depends only upon the distribution of overall chain orientations, which relaxes diffusively. As a result, the linear response $\mu(t)$ can be approximated for such chains in all concentration regimes as an exponentially decaying function

$$\mu(t) \propto A\rho e^{-t/\tau_{rod}} \tag{43}$$

with a prefactor proportional to ρ and with a decay time that is same as that which controls the decay of $G_{orient}(t)$. The main difference between the different concentration regimes is thus the difference in the predicted values of τ_{rod}. It should be born in mind, however, that the single-exponential time dependence predicted for both $\mu(t)$ and $G_{orient}(t)$ in the limit of rod-like chains, and the resulting proportionality of these two functions, is valid only for monodisperse solutions.[47]

III. Viscoelastic Response

We now construct a detailed model of linear viscoelastic response in the tightly-entangled regime. In subsection A, we present a calculation of the response of the primitive chain (i.e., coarse-grained) model, which yields results that are valid for frequencies $\omega \lesssim \tau_e^{-1}$. In subsection B, we extend our calculation of $G^*_{tens}(\omega)$ (which dominates $G^*(\omega)$ at high frequencies) to frequencies $\omega \gg \tau_e^{-1}$, by taking into account the rapid Brownian motion of the polymer within the tube. In subsection C, we collect the resulting governing equations for $G^*(\omega)$ and present numerical results. In subsection D, we discuss how our results would be modified by the presence of cross-links between chains.

(A) Primitive Chain Model. In what follows, we calculate separately the contributions $G_{curve}(t)$, $G_{orient}(t)$, and $G_{stress}(t)$ to the dynamic modulus of the primitive chain model by calculating the time dependence of stress following an infinitesimal step deformation. In doing so, it is convenient to separate our calculation of the initial response of each stress contribution to a step deformation, which yields the value of the corresponding modulus at $t = 0$, from the calculation of the subsequent decay of $G(t)$. A calculation of $G_{curve}(0)$ and $G_{orient}(0)$ is given in Appendix C. The "instantaneous" moduli $G_{curve}(0)$, $G_{orient}(0)$, and $G_{tens}(0)$ given below should, however, be understood to be the values obtained at the earliest times accessible to the primitive chain model, i.e., times $t \sim \tau_e^{-1}$, since both $G_{tens}(t)$ and $G_{curve}(t)$ were found in section V of (I) to increase algebraically with decreasing t for $t \ll \tau_e$. The subsequent decay of stress is controlled in this model by two diffusive processes with widely disparate diffusivities: the slow diffusion of the center of mass of the polymer by reptation, with a diffusivity D_{rep}, which controls the relaxation of $G_{curve}(t)$ and $G_{orient}(t)$, and the faster diffusion of excess length, with a diffusivity D_ϕ, which controls the relaxation of $G_{tens}(t)$.

To calculate the time dependence of $\boldsymbol{\sigma}_{curve}(t)$ and $\boldsymbol{\sigma}_{orient}(t)$, it is sufficient to follow the evolution of the scalar and tensor probability distributions

$$f(\mathbf{u},s) \equiv \langle \hat{f}(\mathbf{u},s) \rangle \tag{44}$$

$$\mathbf{F}(\mathbf{u},s) \equiv \langle \mathbf{w}(s)\,\mathbf{w}(s)\,\hat{f}(\mathbf{u},s) \rangle \tag{45}$$

introduced previously in (I), where

$$\hat{f}(\mathbf{u}',s) \equiv \delta(\mathbf{u}(s) - \mathbf{u}') \tag{46}$$

is a probability density operator for the unit tangent vector $\mathbf{u}(s)$ and $\mathbf{w}(s) = \partial\mathbf{u}(s)/\partial s$ is the curvature vector. The decay of anisotropies in f and $\mathbf{F}$ via reptation may be described at all times $t > 0$ by the diffusion equations

$$\left[\frac{\partial}{\partial t} - D_{rep}\frac{\partial^2}{\partial s^2}\right] f(\mathbf{u},s,t) = 0 \tag{47}$$

$$\left[\frac{\partial}{\partial t} - D_{rep}\frac{\partial^2}{\partial s^2}\right] \mathbf{F}(\mathbf{u},s,t) = 0 \tag{48}$$

The semiflexible nature of the chain affects this decay process only through boundary conditions imposed at the chain ends: In an isotropic solution of reptating chains, the rapid destruction and creation of tube segments at the ends of the tube is assumed to guarantee that the curvature (but not necessarily the orientation) of the chain ends will remain equilibrated at all times. This assumption yields boundary conditions

$$\mathbf{F}(\mathbf{u},s)|_{s=0,L} = \frac{1}{L_p a}(\boldsymbol{\delta} - \mathbf{uu}) f(\mathbf{u},s)|_{s=0,L} \tag{49}$$

$$\left.\frac{\partial f(\mathbf{u},s)}{\partial s}\right|_{s=0,L} = \mp\frac{1}{2L_p}\nabla_u^2 f(\mathbf{u},s)\Big|_{s=0,L} \tag{50}$$

in which ∇_u^2 is a Laplacian on the unit sphere. Equation 49 is simply a statement of the fact that the curvature at the ends of the chain must remain perpendicular to $\mathbf{u}$ and exhibit a distribution of values consistent with the equipartition thereom, as in eq I.18. Equation 50 was given previously in ref 36 and is justified in Appendix A.

To calculate $G_{tens}(t)$, we may describe the relaxation of tension $\mathcal{T}(s,t)$ at all times $t > 0$ by a diffusion equation

$$\left[\frac{\partial}{\partial t} - D_\phi\frac{\partial^2}{\partial s^2}\right] \mathcal{T}(s,t) = 0 \tag{51}$$

which is obtained by combining diffusion eq 19 with eq 15 for $\mathcal{T}$, and which must be solved subject to a boundary condition that $\mathcal{T}(s) = 0$ at both chain ends.

(1) Curvature Stress. The initial value of $G_{curve}(t)$ is calculated in Appendix C by using the results of Appendix A to calculate the response of $f(\mathbf{u},s)$ and $\mathbf{F}(\mathbf{u},s)$ to a small, rapid deformation, while assuming an affine deformation of the tube conformation. This calculation yields a value

$$G_{curve}(0) = \frac{7}{5}\frac{\rho T}{L_e} \tag{52}$$

of order T times the number ρ/L_e of entanglement lengths of chain per unit volume of solution.

The time dependence of $G_{curve}(t)$ at times $t > 0$ is conveniently expressed as a product

$$G_{curve}(t) = G_{curve}(0)\,\bar{\chi}(t) \tag{53}$$

The decay function $\bar{\chi}(t)$ may be obtained by an argument similar to that used in the Doi−Edwards (DE) theory

of flexible polymers: We note that the contribution to $\boldsymbol{\sigma}_{\text{curve}}$ of a given segment of tube vanishes once the 1D Brownian motion of the polymer carries either end of the polymer past that tube segment, since such a segment is then immediately replaced with a segment whose curvature is chosen randomly from an equilibrium distribution of values, as described by eq 49, and since it is shown in (I) that the contribution of a segment of chain to $\boldsymbol{\sigma}_{\text{curve}}$ vanishes whenever the distribution of curvatures is equilibrated, even if the distribution of orientations for that segment remains anisotropic.

The function $\bar{\chi}(t)$ is thus given, as in the DE model, by the probability that a randomly chosen segment of polymer has never left the original tube after a time t. The solution of this first-passage problem[33] may be expressed as an integral

$$\bar{\chi}(t) = \int_0^L \frac{\mathrm{d}s}{L}\, \chi(s,t) \tag{54}$$

where $\chi(s,t)$ is the solution of the diffusion equation

$$\left[\frac{\partial}{\partial t} - D_{\text{rep}}\frac{\partial^2}{\partial s^2}\right]\chi(s,t) = 0 \tag{55}$$

with absorbing boundary conditions $\chi(0,t) = \chi(L,t) = 0$ at the chain ends and an initial condition $\chi(s,0) = 1$. The resulting function $\bar{\chi}(t)$ may be expressed[33] as an infinite series

$$\bar{\chi}(t) = \sum_{n\ \text{odd}} \frac{8}{n^2\pi^2}\, \mathrm{e}^{-D_{\text{rep}}\, q_n{}^2 t} \tag{56}$$

where $q_n \equiv n\pi/L$. As in the DE model, this gives a nearly single-exponential decay with the terminal relaxation time τ_{rep} defined in eq 12. The corresponding contribution to the zero-shear viscosity is given by

$$\eta_{0,\text{curve}} = \frac{\pi^2}{12}\, G_{\text{curve}}(0)\tau_{\text{rep}} \tag{57}$$

The time dependence obtained here for $G_{\text{curve}}(t)$ is thus identical, for any value of L/L_{p}, to that obtained for the total elastic stress in the DE model.

(2) Orientational Stress. The initial value of $G_{\text{orient}}(t)$ is also calculated in Appendix C, by calculating the response of $f(\mathbf{u},s)$ to a small step deformation, which yields a value

$$G_{\text{orient}}(0) = \frac{4 + g_{\text{end}}}{5}\,\frac{T\rho}{L} \tag{58}$$

of order T times the number density $c = \rho/L$ of chains, or T per chain. Here, the quantity g_{end} is a function $g_{\text{end}}(\beta) \equiv (\mathrm{e}^{-\beta} - 1)/\beta$ of the ratio $\beta \equiv 3L/L_{\text{p}}$, with limiting values $g_{\text{end}}(0) = -1$ and $g_{\text{end}}(\infty) = 0$. This function takes into account the extent of nonaffine deformation of the chain due to the tangential flow induced during the step deformation, which is necessary to keep the chain length fixed, as discussed in Appendix C. Because $G_{\text{orient}}(t)$ is found to make a signficant contribution to $G(t)$ only for $L \lesssim L_{\text{p}}$, for which $g_{\text{end}} \simeq -1$, we may hereafter approximate

$$G_{\text{orient}}(0) \simeq \frac{3}{5}\,\frac{T\rho}{L} \tag{59}$$

as found previously for rigid rod solutions,[33,43] without significant loss of accuracy.

To calculate the time dependence of $G_{\text{orient}}(t)$, we first rewrite eq I.36 for $\boldsymbol{\sigma}_{\text{orient}}(t)$ in terms of the orientational probability distribution $f(\mathbf{u},s,t)$ as an angular integral

$$\boldsymbol{\sigma}_{\text{orient}}(t) = \frac{3T\rho}{L}\int \mathrm{d}\mathbf{u}\left(\mathbf{uu} - \frac{1}{3}\boldsymbol{\delta}\right) f(\mathbf{u},L,t) \tag{60}$$

Expanding $f(\mathbf{u},s,t)$ in spherical harmonics, as

$$f(\mathbf{u},s,t) = \sum_{lm} f_{lm}(s,t)\, Y_{lm}(\mathbf{u}) \tag{61}$$

then yields an expansion of $\boldsymbol{\sigma}_{\text{orient}}(t)$ as

$$\boldsymbol{\sigma}_{\text{orient}}(t) = \frac{3T\rho}{L}\sum_{lm} f_{lm}(L,t)\int \mathrm{d}\mathbf{u}\left(\mathbf{uu} - \frac{1}{3}\boldsymbol{\delta}\right) Y_{lm}(\mathbf{u}) \tag{62}$$

We then note that, because $\mathbf{uu} - {}^1/_3\boldsymbol{\delta}$ is an irreducible rank-2 tensor, the angular integral in eq 62 is nonzero only for the $l = 2$ spherical harmonic components, so that $\boldsymbol{\sigma}_{\text{orient}}(t)$ depends only upon the amplitudes of the $l = 2$ components of $\mathbf{f}(\mathbf{u}, L)$. If we assume that $f(\mathbf{u},s,t)$ is independent of s at time $t = 0$,[48] we may describe the subsequent time dependence of $f_{lm}(s,t)$ by a product

$$f_{lm}(s,t) \equiv f_{lm}\chi_l(s,t) \tag{63}$$

where f_{lm} is the s-independent value of $f_{lm}(s,0)$, and $\chi_l(s,t)$ is a decay function that satisfies an initial condition $\chi_l(s,0) = 1$. The modulus $G_{\text{orient}}(t)$ may then be reexpressed as a product

$$G_{\text{orient}}(t) = G_{\text{orient}}(0)\,\chi_2(L,t) \tag{64}$$

containing the decay function for the $l = 2$ components of $f(\mathbf{u},s,t)$ at either end of the chain.

The time dependence of the functions $\chi_{lm}(s,t)$ may be calculated by applying the spherical harmonic expansion 61 both to diffusion eq 47 and boundary condition 50, to show that $\chi_{lm}(s,t)$ is the solution of the diffusion equation

$$\left[\frac{\partial}{\partial t} - D_{\text{rep}}\frac{\partial^2}{\partial s^2}\right]\chi_l(s,t) = 0 \tag{65}$$

subject to boundary conditions

$$\left.\frac{\partial\chi_l(s,t)}{\partial s}\right|_{s=0,L} = \pm\frac{l(l+1)}{2L_{\text{p}}}\chi_l(s,t)\Big|_{s=0,L} \tag{66}$$

with an initial condition $\chi_l(s,0) = 1$. An exact solution of the above may be given, for any value of l or L/L_{p}, as an infinite series[36]

$$\chi_l(s,t) = \sum_{k=1}^{\infty} \frac{4\sin(q_{lk}\,L/2)}{q_{lk}\,L + \sin(q_{lk}\,L)}\cos(q_{lk}s')\mathrm{e}^{-D_{\text{rep}}\,q_{lk}{}^2 t} \tag{67}$$

where $s' \equiv s - L/2$ and where the wavenumbers q_{lk} are the solutions of

$$q_{lk}\tan(q_{lk}\,L/2) = l(l+1)/2L_{\text{p}} \tag{68}$$

indexed by integers $k = 1, 2, 3, \ldots$.

One measure of the relative importance of orientational and curvature stresses is obtained by comparing their contributions to the zero-shear viscosity. To calculate $\eta_{0,\mathrm{orient}}$, we consider the decay of the average

$$\bar{f}(\mathbf{u},t) \equiv \int_0^L \frac{\mathrm{d}s}{L} f(\mathbf{u},s,t) \tag{69}$$

of $f(\mathbf{u},s,t)$ over the length of the chain and of the corresponding averages

$$\bar{\chi}_l(t) \equiv \int_0^L \frac{\mathrm{d}s}{L} \chi_l(s,t) \tag{70}$$

of the decay functions for the angular momentum l components of $\bar{f}(\mathbf{u},t)$. By integrating diffusion eq 65 with respect to s, and then imposing boundary condition 66, we obtain a useful relation

$$\frac{\partial \bar{\chi}_l(t)}{\partial t} = -l(l+1)\frac{D_{\mathrm{rep}}}{LL_{\mathrm{p}}}\chi_l(L,t) \tag{71}$$

between the time derivative of $\bar{\chi}_l(t)$ and the value of $\chi_l(s,t)$ at the chain ends. In deriving eq 71, we have assumed that $\chi_l(0,t) = \chi_l(L,t)$ by symmetry. By integrating eq 71 for the $l = 2$ component from $t = 0$ to $t = \infty$, we may then obtain an expression for $\eta_{0,\mathrm{orient}} \equiv \int_0^\infty \mathrm{d}t\, G_{\mathrm{orient}}(t)$ as

$$\eta_{0,\mathrm{orient}} = G_{\mathrm{orient}}(0)\frac{LL_{\mathrm{p}}}{6D_{\mathrm{rep}}} \tag{72}$$

which is valid for any value of L/L_{p}. Upon comparing eq 72 to eq 57 for $\eta_{0,\mathrm{curve}}$, we find that $\eta_{0,\mathrm{orient}} > \eta_{0,\mathrm{curve}}$ only for rather short rods, of length

$$L < [CL_{\mathrm{p}}L_{\mathrm{e}}]^{1/2} \tag{73}$$

where $C = 2(4 + g_{\mathrm{end}})/7 \simeq 6/7$. This criterion defines a line in parameter space that roughly bisects the rod-like, tightly-entangled regime in Figure 1 of (I), which is defined by the requirement that $L_{\mathrm{e}} \lesssim L \lesssim L_{\mathrm{p}}$. For all chains of length $L \gtrsim [L_{\mathrm{p}}L_{\mathrm{e}}]^{1/2}$, η_0 is instead dominated by $\eta_{0,\mathrm{curve}}$.

It has been found previously[34−36] that the time dependence of $f(\mathbf{u},s,t)$ may be described in this tightly-entangled rod-like limit by a diffusion equation describing rotation of the molecule as a whole, with an effective diffusion constant that depends upon L_{p}. To show this, we first note that, because in this limit $\mathbf{u}(s)$ can vary only slightly with s, the probability density $f(\mathbf{u},s,t)$ must also become almost independent of s. We may thus approximate $f(\mathbf{u},s,t)$ by the average $\bar{f}(\mathbf{u},t)$, and, similarly, approximate

$$\lim_{L \ll L_{\mathrm{p}}} \chi_l(s,t) \simeq \bar{\chi}_l(t) \tag{74}$$

Upon using this approximation in eq 71, we obtain a closed equation for $\bar{\chi}_l(t)$ as

$$\left[\frac{\partial}{\partial t} + l(l+1)\frac{D_{\mathrm{rep}}}{LL_{\mathrm{p}}}\right]\bar{\chi}_l(t) \simeq 0 \tag{75}$$

which is recognizable as the spherical harmonic expansion of the rotational diffusion equation

$$\left[\frac{\partial}{\partial t} - D_{\mathrm{rod}}\frac{\partial^2}{\partial \mathbf{u}^2}\right]\bar{f}(\mathbf{u},t) \simeq 0 \tag{76}$$

with an effective rotational diffusivity

$$D_{\mathrm{rod}} = D_{\mathrm{rep}}/LL_{\mathrm{p}} \tag{77}$$

Using eq 75 to calculate $\bar{\chi}_2(L,t)$ then yields a simple exponential decay

$$\lim_{L \ll L_{\mathrm{p}}} G_{\mathrm{orient}}(t) \simeq \frac{3}{5}\frac{\rho T}{L}\mathrm{e}^{-t/\tau_{\mathrm{rod}}} \tag{78}$$

with the decay time $\tau_{\mathrm{rod}} = 1/(6D_{\mathrm{rod}})$ given in eq 14.

(3) Tension Stress. The tension stress is obtained below by solving diffusion eq 51 for $\mathcal{T}(s,t)$, subject to an initial condition that depends upon the conformation of the chain before deformation and averaging the resulting stress over an equilibrium distribution of initial chain conformations.

Following Maggs,[27] the solution of the diffusion eq 51 for $\mathcal{T}$ along a tube of specified conformation (which, for this purpose, may be regarded as stationary) may be expressed as an integral

$$\mathcal{T}(s,t) = \int_0^L \mathrm{d}s\, G(s,s',t)\, \mathcal{T}(s,0) \tag{79}$$

in which G is the Green's function solution of

$$\left[\frac{\partial}{\partial t} - D_\phi\frac{\partial^2}{\partial s^2}\right]G(s,s',t) = 0 \tag{80}$$

with an initial value $G(s,s',0) = \delta(s - s')$ and absorbing boundary conditions at $s = 0$ and $s = L$. The initial value $\mathcal{T}(s,0)$ after an infinitesimal step deformation is given by eqs 15 and 16, which yield $\mathcal{T}(s,0) = B\delta\boldsymbol{\epsilon}:\mathbf{u}(s)\,\mathbf{u}(s)$, where $\mathbf{u}(s)$ may be taken for the purpose of calculating linear response to be the value of $\mathbf{u}$ immediately before deformation. Substituting eq 79 for $\mathcal{T}(s,t)$, with this initial condition, into definition I.37 for $\boldsymbol{\sigma}_{\mathrm{tens}}$ yields a stress contribution

$$\boldsymbol{\sigma}_{\mathrm{tens}}(t) = \frac{\rho B}{L}\int_0^L \mathrm{d}s \int_0^L \mathrm{d}s'\, G(s,s',t) \times \langle \mathbf{u}(s)\,\mathbf{u}(s)\,\mathbf{u}(s')\,\mathbf{u}(s')\rangle_{\mathrm{eq}}:\delta\boldsymbol{\epsilon} \tag{81}$$

where $\langle\ldots\rangle_{\mathrm{eq}}$ denotes an average over the thermal equilibrium distribution of chain conformations. By using eq A4 to evaluate this equilibrium average, and assuming a volume-preserving deformation, with $\boldsymbol{\delta}:\delta\boldsymbol{\epsilon} = 0$, we obtain a stress of the form $\boldsymbol{\sigma}_{\mathrm{tens}}(t) = G_{\mathrm{tens}}(t)(\delta\boldsymbol{\epsilon} + \delta\boldsymbol{\epsilon}^{\dagger})$, with a dynamic modulus

$$G_{\mathrm{tens}}(t) = G_{\mathrm{tens}}(0)\,\psi(t) \tag{82}$$

in which

$$G_{\mathrm{tens}}(0) = \frac{1}{15}\rho B \tag{83}$$

is the initial value of $G_{\mathrm{tens}}(t)$, and

$$\psi(t) = \frac{1}{L}\int_0^L \mathrm{d}s \int_0^L \mathrm{d}s'\, G(s,s',t)\, \mathrm{e}^{-3|s-s'|/L_{\mathrm{p}}} \tag{84}$$

is a decay function with initial value $\psi(0) = 1$.

A series expansion for $\psi(t)$ may be obtained by Fourier expanding $G(s,s',t)$ in eq 84 as

$$G(s,s',t) = \frac{2}{L}\sum_{n=1}^{\infty}\sin(q_n s)\sin(q_n s')\, e^{-D_\phi q_n^2 t} \quad (85)$$

where $q_n \equiv n\pi/L$. Integrating with respect to s and s' then yields

$$\psi(t) = \sum_{n=1}^{\infty}\psi_n(\beta)\, e^{-D_\phi q_n^2 t} \quad (86)$$

$$\psi_n(\beta) \equiv 2\frac{\beta^3 + q_n^2 L^2[\beta + 2 - 2(-1)^n e^{-\beta}]}{(q_n^2 L^2 + \beta^2)^2} \quad (87)$$

where $\beta \equiv 3L/L_p$. Below, we discuss separately the limiting behaviors obtained for coil-like and rod-like chains.

We consider first the limit of coil-like chains, with $L \gg L_p$. In this limit, $\psi(t)$ is shown below to exhibit three time regimes: At times $t \ll \tau_{\phi p}$, excess length has not had time to diffuse a distance L_p, and $\psi(t) \simeq 1$. At times $\tau_{\phi L} \gg t \gg \tau_{\phi p}$, excess length has had time to diffuse distances longer than L_p but shorter than the length of the chain, and $\psi(t)$ is found to decay as $\psi(t) \propto t^{-1/2}$. At times $t \gg \tau_{\phi L}$, excess length has had time to diffuse to the ends of the chain, and $\psi(t)$ is found to decay exponentially with a decay time $\tau_{\phi L}$.

At all times $t \ll \tau_{\phi L}$, an approximate expression for $\psi(t)$ may be obtained by taking the limits of integration to infinity in eq 84, giving

$$\psi(t) \simeq \int_{-\infty}^{+\infty} dS\, G(S,t)\, e^{-3|S|/L_p} \quad (88)$$

where $S \equiv s - s'$ and where $G(S,t) = e^{-S^2/(4D_\phi t)}/(4\pi D_\phi t)^{1/2}$ is the Greens' function for diffusion on an infinite domain. The above integral may be evaluated to obtain

$$\psi(t) \simeq e^{t/\tau_{\phi p}}\,\mathrm{erfc}([t/\tau_{\phi p}]^{1/2}) \quad (89)$$

in which $\tau_{\phi p}$ is defined in eq 21. The limiting forms of $\psi(t)$ for short and intermediate times are

$$\psi(t) \sim \begin{cases} 1 & t \ll \tau_{\phi p} \\ (\pi t/\tau_{\phi p})^{-1/2} & \tau_{\phi p} \ll t \ll \tau_{\phi L} \end{cases} \quad (90)$$

giving $G_{tens}(t) \propto t^{-1/2}$ at intermediate times. The Fourier transform of eq 89 may be evaluated to obtain a corresponding approximation

$$\psi^*(\omega) \simeq \frac{i\omega - [i\omega\tau_{\phi p}^{-1}]^{1/2}}{i\omega - \tau_{\phi p}^{-1}} \quad (91)$$

for the function $\psi^*(\omega) \equiv i\omega \int_0^\infty dt\, e^{-i\omega t}\psi(t)$, which is valid for frequencies $\omega \gg \tau_{\phi L}^{-1}$. The corresponding limiting forms of $\psi^*(\omega)$ at high and intermediate frequencies are

$$\psi^*(\omega) \sim \begin{cases} (i\omega\tau_{\phi p})^{1/2} & \tau_{\phi L}^{-1} \ll \omega \ll \tau_{\phi p}^{-1} \\ 1 & \tau_{\phi p}^{-1} \ll \omega \end{cases} \quad (92)$$

This behavior yields a complex modulus that varies as $G^*_{tens}(\omega) \propto (i\omega)^{1/2}$ at intermediate frequencies and that can exhibit an elastic plateau at frequencies $\tau_{\phi p}^{-1} \lesssim \omega \lesssim \tau_e^{-1}$, if $\tau_e \ll \tau_{\phi p}$.

At times $t \gg \tau_{\phi L}$, $\psi(t)$ instead exhibits an exponential decay dominated by the slowest decaying mode in eq 87. Correspondingly, $G^*_{tens}(\omega)$ exhibits fluidlike terminal behavior at frequencies $\omega \ll \tau_{\phi L}^{-1}$, with $G''_{tens}(\omega) \simeq i\omega\eta_{0,tens}$. The corresponding contribution to η_0 is

$$\lim_{L \gg L_p} \eta_{0,tens} \simeq \frac{1}{135}\rho\zeta L L_p \quad (93)$$

This is smaller than eq 57 for $\eta_{0,curve}$ by a factor of order $L_p L_e/L^2$, so the curvature stress dominates η_0 throughout the coil-like regime.

We now consider the limit of rod-like chains, with $L \ll L_p$. Here, an approximate expression for $\psi(t)$ at all times may be obtained by approximating the factor of $e^{-3|s-s'|/L_p}$ in eq 84 by unity, giving

$$\psi(t) \simeq \frac{1}{L}\int_0^L ds \int_0^L ds'\, G(s,s',t) \quad (94)$$

Using eq 85 for $G(s,s',t)$ and carrying out the integration with respect to s and s' then yields a decay function

$$\psi(t) \simeq \sum_{n\ \mathrm{odd}} \frac{8}{n^2\pi^2} e^{-D_\phi q_n^2 t} \quad (95)$$

with $q_n = n\pi/L$. Equation 95 is of the same functional form as eq 56 for $\bar{\chi}(t)$, with the diffusivity D_{rep} simply replaced by D_ϕ. This is because both functions describe the decay of stress due to a diffusive process (i.e., reptation or diffusion of excess length) that may be formulated in terms of a diffusion equation with an s-independent initial condition and absorbing boundary conditions at both ends of the chain.

The tension contribution to η_0 in the rod-like limit is

$$\lim_{L \ll L_p} \eta_{0,tens} \simeq \frac{1}{180}\rho\zeta L^2 \quad (96)$$

which is smaller than eq 57 for $\eta_{0,curve}$ by a factor of L_e/L. It is straightforward to show that eq 96 for $\eta_{0,tens}$ is numerically identical to the "viscous" contribution[33] to the viscosity of a solution of free-draining rigid rods that arise from the contributions of tangential constraint forces that act to prevent stretching or compression of the rods.[33,43] As shown in Figure 3, this results in all concentration regimes in a terminal regime for $G^*_{tens}(\omega)$ in which $G^*_{tens}(\omega) \simeq i\omega\eta_{0,tens}$, and in which $\eta_{0,tens}/\rho$ takes on the same numerical value, given by eq 96, in all concentration regimes. This terminal regime occurs at frequencies $\omega \ll \tau_{\phi L}^{-1}$ for tightly-entangled rods with $L_p \gg L \gtrsim [L_p L_e]^{1/2}$ and at $\omega \ll \tau_{||}^{-1}$ for tightly-entangled rods with $L \lesssim [L_p L_e]^{1/2}$, as well as for loosely-entangled and dilute rods.

B. High-Frequency Response. We now extend our calculation of $G^*(\omega)$ to frequencies $\omega \gg \tau_e^{-1}$, for which the frequency dependence of $G^*(\omega)$ is controlled by the relaxation of transverse undulations of the polymer within the tube with wavelengths less than L_e. We assume, based on arguments given in section V of (I), that in this regime $G^*(\omega)$ will be dominated by $G^*_{tens}(\omega)$, so we focus exclusively on extending the calculation of $G^*_{tens}(\omega)$.

For this purpose, it is convenient to consider the stress induced in a solution undergoing a small oscillatory deformation with frequency ω, rather than the time-

dependent response to a step strain, and to introduce the temporal Fourier transform

$$\delta\hat{\epsilon}(\omega) \equiv \int_{-\infty}^{+\infty} dt\ e^{-i\omega t}\ \delta\epsilon(t) \tag{97}$$

of the strain and other variables, hereafter indicating Fourier transformed variables by the use of a caret.

To calculate $G^*_{tens}(\omega)$, we consider the oscillatory response of the tension $\hat{\mathcal{T}}(s,\omega)$ along a chain confined within a tube, while assuming that the tube undergoes an oscillatory affine deformation. The calculation of the stress is based upon the assumption that there exists some frequency-dependent linear relationship between the average tension $\langle\hat{\mathcal{T}}(s,\omega)\rangle$ induced in the chain and the corresponding fluctuation $\hat{\phi}(s,\omega)$ in the average contour length density, of the form

$$\langle\hat{\mathcal{T}}(s,\omega)\rangle \simeq \hat{B}(\omega)\ \hat{\phi}(s,\omega)/\phi_{eq} \tag{98}$$

for all $\omega \neq 0$. The static modulus B used in the previous subsection is given by the low-frequency limit $B = \hat{B}(\omega\rightarrow 0)$. In what follows, $\hat{B}(\omega)$ is found to remain near $\hat{B}(0)$ for all $\omega \ll \tau_e^{-1}$ but to increase algebraically with ω for $\omega \gg \tau_e^{-1}$. Here and in what follows, we use $\langle ...\rangle$ to indicate an average over the Brownian fluctuations of the polymer within the tube, while assuming the motion of the tube conformation to be deterministic.

The only physical approximation made in our use of eq 98 is the assumption that the linear response function relating $\phi(s,\omega)$ and $\hat{\mathcal{T}}(s',\omega)$ may taken to be local in s, rather than requiring the use of a more general nonlocal kernel relating the response at point s to perturbations at points $s' \neq s$. This approximation is justified by the observation that the correlations in the values of $\hat{\mathcal{T}}(s,\omega)$ at points s and s' are expected to extend over distances $|s - s'|$ of order L_p (for $L \gg L_p$) or L (for $L \ll L_p$), while any nonlocalities in the response of a confined chain to an inhomogenous tension are expected to extend only over much shorter distances, of order L_e.

The calculation proceeds in three steps. In III.B.1, we derive an expression for $G^*_{tens}(\omega)$ in terms of the initially unknown response function $\hat{B}(\omega)$. In III.B.2, we construct a Langevin equation for an inextensible polymer in a tube undergoing oscillatory deformation, in order to show how affine deformation of the tube affects motion of the polymer within the tube. In III.B.3, we actually calculate $\hat{B}(\omega)$.

(1) Tension Stress. As in the primitive chain model, we assume here that ϕ may relax only via the tension-driven tangential motion of the polymer. By repeating the arguments leading to diffusion eq 19, while now allowing for the existence of a frequency-dependent modulus $\hat{B}(\omega)$, it is straightforward to show that $\hat{\phi}(s,\omega)$ obeys a Fourier transformed diffusion equation

$$\left[i\omega - \hat{D}_\phi(\omega)\frac{\partial^2}{\partial s^2}\right]\hat{\phi}(s,\omega) = -\phi_{eq}\hat{\kappa}(\omega):\mathbf{u}(s)\ \mathbf{u}(s) \tag{99}$$

where

$$\hat{D}_\phi(\omega) \simeq \hat{B}(\omega)/\zeta \tag{100}$$

is a frequency-dependent diffusivity, and $\hat{\kappa}(\omega) \equiv i\omega\delta\hat{\epsilon}(\omega)$ is the Fourier transform of the rate of deformation tensor $\kappa(t) \equiv d(\delta\epsilon(t))/dt$. The right hand side of eq 99 takes into account the oscillatory stretching and compression of each tube segment due to the affine deformation of the tube, as discussed in Appendix B.

As in the primitive chain model, the solution of diffusion eq 99 may be expressed as a functional

$$\hat{\phi}(s,\omega) = -\phi_{eq}\int_0^L ds'\ \hat{G}(s,s',\omega)\ \hat{\kappa}(\omega):\mathbf{u}(s')\ \mathbf{u}(s') \tag{101}$$

in which $\hat{G}(s,s',\omega)$ is the Green's function solution of eq 99 with boundary conditions $\hat{\phi}(s,\omega)$ for $s = 0$, L and $\omega \neq 0$. This Fourier transformed Green's function may be written explicitly as a sum

$$\hat{G}(s,s',\omega) = \frac{2}{L}\sum_{n=1}^{\infty}\frac{\sin(q_n s)\ \sin(q_n s')}{i\omega + D_\phi(\omega)q_n^{\ 2}} \tag{102}$$

which is a straightforward generalization of eq 85. By using eq 101 for $\hat{\phi}(s,\omega)$ to calculate the contribution to $\hat{\boldsymbol{\sigma}}_{tens}(\omega)$ from a tube of specified conformation and then averaging over an equilibrium distribution of tube conformations, we obtain a modulus of the form

$$G^*_{tens}(\omega) = \frac{1}{15}\rho\hat{B}(\omega)\ \psi^*(\omega) \tag{103}$$

where

$$\psi^*(\omega) \equiv \frac{i\omega}{L}\int_0^L ds\int_0^L ds'\ \hat{G}(s,s',\omega)\ e^{-3|s-s'|/L_p} \tag{104}$$

describes the effects of tangential diffusion. Note that this final result for $G^*_{tens}(\omega)$ may be obtained by simply replacing the static modulus B by a frequency-dependent modulus $\hat{B}(\omega)$ throughout our previous calculation of $G^*_{tens}(\omega)$.

The frequency dependence of the function $\psi^*(\omega)$ is found to closely approach that found in the primitive chain model whenever the dominant decay times for the diffusion of tension remain longer than τ_e, since in this case the values of $\hat{B}(\omega)$ evaluated at the corresponding frequencies approach the static value $B = \hat{B}(0)$ used in the primitive chain model. As discussed in section II, this is found to be the case for all chains of length $L \gtrsim [L_e L_p]^{1/2}$. Results for the function $\psi^*(\omega)$ calculated using eqs 102 and 104 thus differ signficantly from those obtained in the primitive chain model only in the case of short rods, of length $L \lesssim [L_e L_p]^{1/2}$, for which the tension relaxes in a decay time $\tau_{||} < \tau_e$.

At sufficiently high frequencies, above the highest decay rate for the diffusive relaxation of tension, the tangential friction becomes effective in preventing tangential slippage of the polymer along the tube, thus enforcing an affine tangential deformation of the chain, and giving $\psi^*(\omega) \simeq 1$. This high-frequency limit is obtained for $\omega \gg \tau_{\phi p}^{-1}$ for $L \gg L_p$, for $\omega \gg \tau_{\phi L}^{-1}$ for $L_p \gtrsim L \gtrsim [L_e L_p]^{1/2}$, and for $\omega \gg \tau_{||}^{-1}$ for $L \lesssim [L_e L_p]^{1/2}$. In this high-frequency regime, we may approximate $\psi^*(\omega) \simeq 1$, giving a modulus

$$G^*_{tens}(\omega) \simeq \frac{1}{15}\rho\hat{B}(\omega) \tag{105}$$

(2) Langevin Equation. In what follows, we consider the high-frequency Brownian motion of a polymer confined within a tube, in which the tube contour is assumed to undergo an small, oscillatory affine deformation. We consider a short segment of tube, of length much less than L_p, within a solution that is subjected

to an oscillatory strain $\delta\epsilon(t)$. We denote the instantaneous orientation of the segment of interest at time t by a unit vector $\mathbf{u}(t)$. This instantaneous tube tangent may be expressed to first order in $\delta\epsilon(t)$ as a sum $\mathbf{u}(t) = \bar{\mathbf{u}} + (\boldsymbol{\delta} - \bar{\mathbf{u}}\bar{\mathbf{u}})\cdot\delta\epsilon(t)$, where $\bar{\mathbf{u}}$ is the time average of the segment orientation over one cycle of the deformation. We parametrize the position $\mathbf{r}(s,t)$ of a specified "monomer" by a sum

$$\mathbf{r}(s,t) = (s + f(s,t))\mathbf{u}(t) + \mathbf{h}(s,t) \tag{106}$$

where $f(s,t)$ is a displacement along the tube tangent $\mathbf{u}(t)$, $\mathbf{h}(s,t)$ is a normal displacement that is defined so that $\mathbf{h}(s,t)\cdot\mathbf{u}(t) = 0$, and s is the position of the average position of this monomer, relative to some arbitrary point on the tube, as measured along the undeformed tube contour.

The average contour length density $\phi(t)$ within the segment is given by

$$\phi(t) = \left\langle \left[1 + \left| \frac{\partial \mathbf{h}(s,t)}{\partial s} \right|^2 \right]^{1/2} \right\rangle \tag{107}$$

evaluated at any point s within the segment. The deviation $\delta\phi(t) = \phi(t) - \phi_{eq}$ of $\phi(t)$ from its equilibrium value is given to harmonic order in $\mathbf{h}$ by

$$\delta\phi(t) \simeq \frac{1}{2}\left\{ \left\langle \left| \frac{\partial \mathbf{h}}{\partial s} \right|^2 \right\rangle - \left\langle \left| \frac{\partial \mathbf{h}}{\partial s} \right|^2 \right\rangle_{eq} \right\} \tag{108}$$

where $\langle ... \rangle_{eq}$ denotes an average over Brownian fluctuations evaluated in the absence of any macroscopic strain. Because the chain is inextensible, $\mathbf{r}(s,t)$ must satisfy the local constraint $|\partial\mathbf{r}(s,t)/\partial s|^2 = \phi_{eq}^2$ (where the factor of ϕ_{eq}^2 arises from the fact that s is being measured along the tube rather than along the chain), which may be expanded to linear order in f and harmonic order in $\mathbf{h}$ to obtain a corresponding constraint

$$\frac{\partial f}{\partial s} \simeq -\frac{1}{2}\left\{ \left| \frac{\partial \mathbf{h}}{\partial s} \right|^2 - \left\langle \left| \frac{\partial \mathbf{h}}{\partial s} \right|^2 \right\rangle_{eq} \right\} \tag{109}$$

which must hold for all s.

To approximate the confinement of the polymer to a tube, we assume an effective single-chain potential energy of the form

$$U_{eff} \simeq \frac{1}{2} T L_p \int ds \left\{ \left| \frac{\partial^2 \mathbf{h}}{\partial s^2} \right|^2 + q_e^4 \left| \mathbf{h} \right|^2 \right\} \tag{110}$$

which is the sum of the intramolecular bending energy and a harmonic confining potential. Here, q_e is a phenomological parameter of order $1/L_e$ whose value determines the magnitude of the confining potential. In (I), we use the same model to derive quantitative approximations for L_e, $\hat{B}(0)$, and D_e as functions of q_e and L_p.

The Brownian motion of an inextensible chain in such a potential may be described by a Langevin equation of the form

$$\boldsymbol{\zeta}\cdot\left(\frac{\partial \mathbf{r}}{\partial t} - \boldsymbol{\kappa}\cdot\mathbf{r} \right) = -\frac{\delta U_{eff}}{\delta \mathbf{r}} + \frac{\partial}{\partial s}\left(\mathscr{T} \frac{\partial \mathbf{r}}{\partial s} \right) + \mathbf{f} \tag{111}$$

Here, $\mathscr{T}(s,t)$ is a microscopic tension that must be chosen so as to satisfy constraint 110, $\boldsymbol{\zeta}$ is a local coefficient-of-friction tensor of the form $\boldsymbol{\zeta} = \zeta\mathbf{u}\mathbf{u} + \zeta_\perp(\boldsymbol{\delta} - \mathbf{u}\mathbf{u})$, with different friction coefficients for motion parallel and perpendicular to $\mathbf{u}(t)$, and $\mathbf{f}(s,t)$ is a random force with a variance $\langle \mathbf{f}(s,t)\,\mathbf{f}(s',t') \rangle \simeq 2T\zeta\delta(s - s')\,\delta(t - t')$ and a vanishing mean value. By expanding eq 111 to lowest nontrivial order in f, $\mathbf{h}$, and $\delta\epsilon$, we may obtain a pair of approximate equations

$$\zeta\left\{ \frac{\partial f}{\partial t} - s\boldsymbol{\kappa}:\mathbf{u}\mathbf{u} \right\} \simeq \frac{\partial \mathscr{T}}{\partial s} + f_{\parallel} \tag{112}$$

$$\zeta_\perp \frac{\partial \mathbf{h}}{\partial t} \simeq -\frac{\delta U}{\delta \mathbf{h}} + \frac{\partial}{\partial s}\left(\mathscr{T} \frac{\partial \mathbf{h}}{\partial s} \right) + \mathbf{f}_\perp \tag{113}$$

for motions parallel to and perpendicular to $\mathbf{u}$, in which $f_\parallel$ and $\mathbf{f}_\perp$ are the parallel and perpendicular components of the Langevin noise. To the level of approximation used here, these equations are coupled only by the appearance of $\mathscr{T}$ in both equations.

In order to connect eqs 112 and 113 to our diffusion equation for the tension, we may note that eq 112 is simply a restatement of the tangential force balance given in eq 18, modified to take into account the presence of random tangential forces, in which $\nu(s) = \partial f/\partial t - s\boldsymbol{\kappa}:\mathbf{u}\mathbf{u}$ is the local tangential velocity of the polymer relative to the tube. Upon averaging eq 112 over possible values of the Brownian forces, differentiating both sides with respect to s, and using eqs 109 and 110 to relate $\langle \partial f/\partial s \rangle$ to $\phi(s)$, we obtain an average tangential force balance

$$\zeta\left\{ \frac{\partial \phi}{\partial t} + \boldsymbol{\kappa}:\mathbf{u}\mathbf{u} \right\} \simeq -\frac{\partial^2 \langle \mathscr{T} \rangle}{\partial s^2} \tag{114}$$

If we assume the existence of a local linear relationship between $\langle \mathscr{T} \rangle$ and ϕ, and Fourier transform with respect to time, then, to lowest nontrivial order in $\langle |\partial\mathbf{h}/\partial s|^2 \rangle$, we recover eq 99.

(3) Calculation of $\hat{B}(\omega)$. To calculate $\hat{B}(\omega)$, we now use eq 113, the transverse component of the microscopic equation of motion, to calculate the dynamic linear response of $\delta\phi(t)$ to an applied tension $\mathscr{T}(t)$. For this purpose, we may ignore the stochastic fluctuations of $\mathscr{T}(s,t)$ and calculate the response to a sinusoidally oscillating, s-independent applied tension $\mathscr{T}(t)$.

To begin, we Fourier transform eq 113 with respect to s to obtain a set of decoupled Langevin equations

$$\frac{\partial \mathbf{h}(q,t)}{\partial t} \simeq -\{K(q) + \mathscr{T}(t)q^2\}\mathbf{h}(q,t) + \mathbf{f}_\perp(q,t) \tag{115}$$

for the Fourier mode amplitudes $\mathbf{h}(q,t) \equiv \int ds\ \mathbf{h}(s,t)\, e^{iqs}$ of the normal displacment field, where $\mathbf{f}_\perp(q,t)$ is the corresponding Fourier mode amplitude of $\mathbf{f}_\perp(s,t)$ and where $K(q) = TL_p(q^4 + q_e^4)$ is an effective spring constant for a mode of wavenumber q in the absence of tension. Similarly, we expand eq 108 for $\delta\phi(t)$ as

$$\delta\phi(t) \simeq \int \frac{dq}{2\pi}\, q^2 a(q,t) \tag{116}$$

where we define

$$a(q,t) \equiv {}^1/_2\{\langle |\mathbf{h}(q,t)|^2 \rangle - \langle |\mathbf{h}(q,t)|^2 \rangle_{eq}\} \tag{117}$$

If we then describe the linear response of the temporal Fourier transform $\hat{a}(q,\omega)$ of $a(q,t)$ by an unknown response function $\hat{F}(q,\omega)$, such that

$$\hat{a}(q,\omega) = -q^2 \hat{F}(q,\omega)\ \hat{\mathscr{T}}(\omega) \tag{118}$$

we obtain an integral expression

$$\hat{B}(\omega) = \left\{ \int \frac{dq}{2\pi} q^2 \hat{F}(q,\omega) \right\}^{-1} \tag{119}$$

for the modulus $\hat{B}(\omega) \equiv \hat{\mathcal{T}}(\omega)/\hat{\phi}(\omega)$.

The calculation of $F(q,t)$ amounts to the calculation of the transient response of the mean-squared amplitude of a Brownian harmonic oscillator to a time-dependent shift in the oscillator spring constant. This may be calculated by several methods, which yield an exponential time dependence

$$F(q,t) = \frac{2\zeta_\perp T}{K(q)} e^{-2K(q)t/\zeta_\perp} \tag{120}$$

with a decay time half that of the oscillator, or a corresponding frequency dependence

$$\hat{F}(q,\omega) = \frac{T}{K(q)} \frac{1}{K(q) + (i/2)\zeta_\perp \omega} \tag{121}$$

Substituting eq 121 into eq 119 then yields

$$\hat{B}(\omega) = \left\{ \int \frac{dq}{2\pi} \frac{T}{K(q)} \frac{q^4}{K(q) + (i/2)\zeta_\perp \omega} \right\}^{-1} \tag{122}$$

as our final result for $\hat{B}(\omega)$.

In the limit $\omega \ll \tau_e^{-1}$, eq 122 yields the static value $B = \hat{B}(0) = 2^{7/2} T L_p q_e^3$ given previously in eqs I.40 and I.41. In the limit $\omega \gg \tau_e^{-1}$, $\hat{B}(\omega)$ instead becomes independent of q_e and exhibits a limiting power law

$$\lim_{\omega \gg \tau_e^{-1}} \hat{B}(\omega) = \frac{2^{3/4} T}{L_p} \left(i\omega \frac{\zeta_\perp L_p^3}{T} \right)^{3/4} \tag{123}$$

in agreeement with the scaling arguments given in section V of (I). An equivalent result for the high-frequency behavior of the autocorrelation function for the end-to-end distance of a nearly straight semiflexible chain, which is related to $\hat{B}(\omega)$ by the fluctuation dissipation theorem, has been obtained by Granek[50] and by Gittes and MacKintosh.[51] Substituting limiting form 123 into eq 105 then yields eq 35 for the high-frequency limiting behavior of $G^*_{tens}(\omega)$, which has also been obtained independently by Gittes and MacKintosh.[51]

C. Results. Our final result for $G^*(\omega)$ is given by adding the results of the primitive chain model of subsection A for $G^*_{curve}(\omega)$ and $G^*_{orient}(\omega)$ to the results of subsection B for $G^*_{tens}(\omega)$. For purposes of numerical calculation, these functions may be expressed as series expansions

$$G^*_{curve}(\omega) = \frac{7}{5} \frac{\rho T}{L_e} \sum_{n\ \mathrm{odd}} \frac{8}{n^2\pi^2} \frac{i\omega}{i\omega + D_{rep} q_n^2}$$

$$G^*_{orient}(\omega) \simeq \frac{3}{5} \frac{\rho T}{L} \sum_{k=1}^{\infty} \frac{2\sin(q_{2k} L)}{q_{2k} L + \sin(q_{2k} L)} \frac{i\omega}{i\omega + D_{rep} q_{2k}^2}$$

$$G^*_{tens}(\omega) = \frac{1}{15} \rho \hat{B}(\omega) \sum_{n=1}^{\infty} \psi_n(\beta) \frac{i\omega}{i\omega + \hat{D}_\phi(\omega) q_n^2} \tag{124}$$

where $q_n = \pi n/L$, q_{2k} is a solution of eq 68 with $l = 2$, the coefficients $\psi_n(\beta)$ are defined in eq 87, and $\hat{D}_\phi(\omega) \equiv \hat{B}(\omega)/\zeta$. The modulus $\hat{B}(\omega)$ is given by eq 122, which is most easily evaluated by applying the method of residues to the Fourier integral and numerically evaluating the resulting sum of residues. The value of L_e is given in eq I.41, using a model identical to that used above to calculate $\hat{B}(\omega)$, which yields $L_e = 2^{3/2} q_e^{-1}$. Values for the friction coefficients ζ and $\zeta_\perp$ are estimated using eqs 9 and 10, in which we use hydrodynamic screening lengths $\xi = \xi_\perp = \rho^{-1/2}$.[49] The input parameters needed to calculate $G^*(\omega)$ for a monodisperse solution are thus: ρ, L, L_p, η_s, the hydrodynamic radius d, and some measure of the tube diameter, as specified by L_e, D_e, or q_e. If L_p, the tube diameter D_e, and the hydrodynamic diameter d can be measured independently, as is true for *F*-actin solutions, then the model has no remaining adjustable parameters.

In Figure 5a–c we show the calculated moduli for monodisperse solutions containing chains of lengths (a) $L = L_p/4$, (b) $L = L_p$, and (c) $L = 10L_p$, for parameter values $L_p = 17\ \mu$m, $\rho = 39\ \mu$m^{-2}, $D_e = 0.2\ \mu$m, and $d = 0.007\ \mu$m, which yield a mesh size $\rho^{-1/2} \simeq 0.16\ \mu$m and an entanglement length $L_e \simeq 2.2\ \mu$m and which are believed to be representative of an *F*-actin solution with a concentration of 1 mg/mL of actin, as discussed in section V. For the system shown in Figure 5b, with $L = L_p$, this yields values

$$G_{orient}(0) \simeq 0.06\ \mathrm{dyn/cm^2}$$

$$G_{curve}(0) \simeq 1.0\ \mathrm{dyn/cm^2}$$

$$G_{tens}(0) \simeq 720\ \mathrm{dyn/cm^2} \tag{125}$$

for the "instantaneous" moduli of the primitive chain model, and relaxation rates

$$\tau_{rep}^{-1} \simeq 0.004\ \mathrm{s^{-1}}$$

$$\tau_{\phi p}^{-1} \simeq 430\ \mathrm{s^{-1}}$$

$$\tau_e^{-1} \simeq 45\ \mathrm{s^{-1}} \tag{126}$$

where $\tau_{\phi p}^{-1}$ has been defined using the zero-frequency limit of $D_\phi(\omega)$.

Because the value of $\tau_{\phi p}^{-1}$ given above (which is similar to $\tau_{\phi L}^{-1}$) is signficantly greater than τ_e^{-1}, no tension-dominated plateau in $G'(\omega)$ can appear for these values of D_e and L_p, even for $L \gg L_p$. The fact that $\tau_{\phi p} < \tau_e$ is somewhat surprising, since scaling arguments given in section II suggest that $\tau_e/\tau_{\phi p} \propto L_e/L_p$, and since $L_p \sim 10L_e$ in this system. This is primarily a consequence of the appearance of a rather large numerical prefactor in eq I.41 for $\hat{B}(0)$, which gives $\hat{B}(0) = 256 T L_p^2/L_e^3$.

Figure 5 shows how $G^*(\omega)$ can evolve with increasing contour length L for a series of monodisperse tightly-entangled solutions with equal concentration ρ. Only in the system of rod-like chains with $L = L_p/4$, shown in Figure 5a, do we see evidence of a non-negligible orientational stress, which shows up as a weak shoulder in $G'(\omega)$ visible at $\omega \simeq 2 \times 10^{-2}\ \mathrm{s^{-1}}$. In the same rod-like system, $G''(\omega)$ varies linearly with ω over a wide range of frequencies $\omega \gtrsim 10$ rad/s (as in a rigid rod solution) and crosses over to its high-frequency asymp-

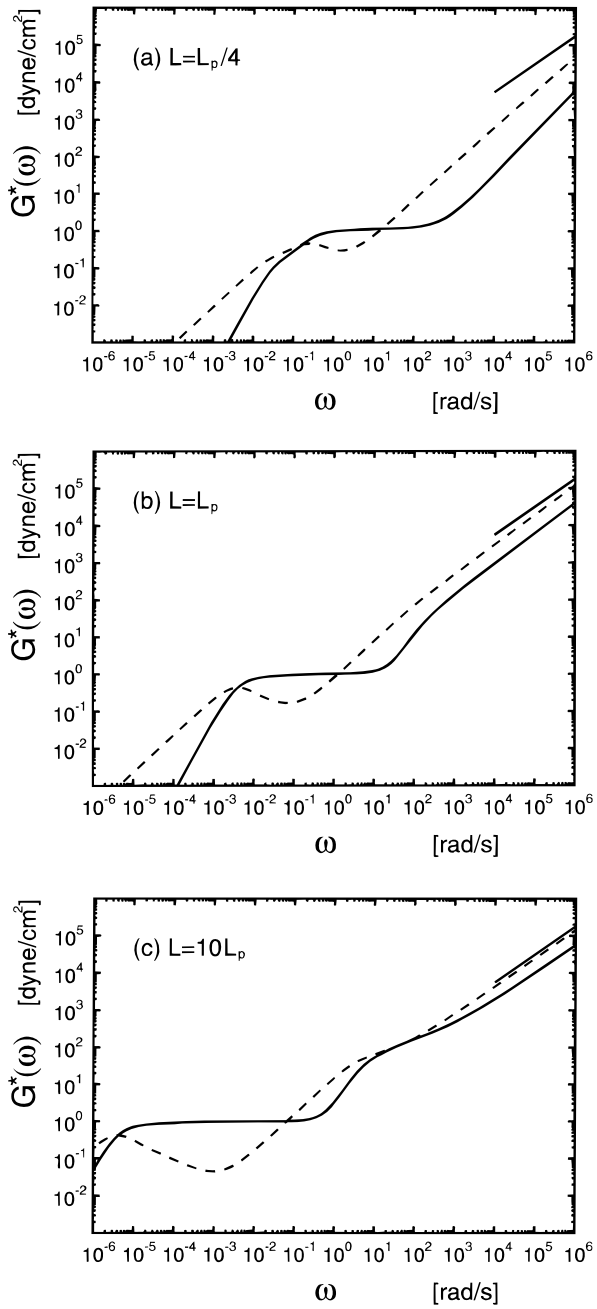

Figure 5. Calculated moduli $G'(\omega)$ (solid line) and $G''(\omega)$ (dotted line) for monodisperse solutions with (a) $L = L/4$, (b) $L = L_p$, and (c) $L = 10L_p$. The remaining parameters are given values: $L_p = 17\ \mu$m, $\rho = 39\ \mu$m^{-2}, $D_e = 0.2\ \mu$m, $L_e \simeq 2.2\ \mu$m, $\eta_s = 0.01$ Poise, and $d = 0.007\ \mu$m, which are believed to be representative of a 1 mg/mL solution of *F*-actin. The straight solid line in each figure has a slope of $^3/_4$ and is the predicted high-frequency asymptote of $G''(\omega)$.

totic behavior of $G''(\omega) \propto \omega^{3/4}$, shown by the straight black line, only above a terminal relaxation frequency for $G^*_{tens}(\omega)$ of $\tau_{||}^{-1} \sim 10^8$ rad/s, which is beyond the range of both the plot and current experiments. If L were reduced significantly below the value of $L_p/4 = 4.25\ \mu$m, L would fall below the estimated entanglement length of $L_e \sim 2\ \mu$m, presumably causing a crossover to the loosely-entangled rod-like regime and a collapse of the curvature-dominated plateau. This crossover cannot be described by the model developed here. As the chain length is instead increased to $L = L_p$ and $L = 10L_p$, as shown in Figure 5b,c, the terminal relaxation

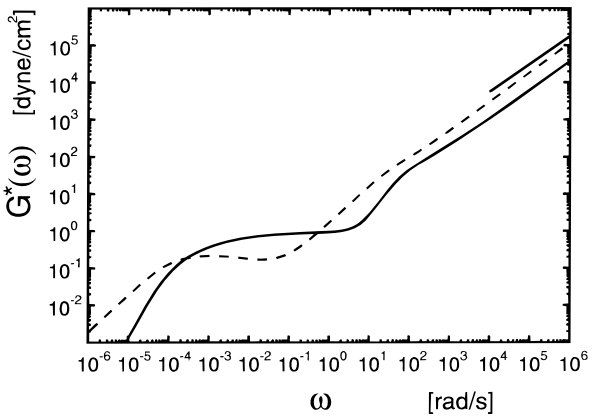

Figure 6. Calculated moduli $G'(\omega)$ (solid line) and $G''(\omega)$ (dotted line) for a polydisperse actin solution with $\bar{L} = 17\ \mu$m and an exponential distribution of chain lengths, for the same values of L_p, ρ, D_e, etc. as those used in Figure 5.

frequency τ_{rep}^{-1} of $G^*_{curve}(\omega)$ rapidly becomes smaller than the terminal frequency of $G^*_{orient}(\omega)$, causing the larger curvature contribution to swamp $G_{orient}(\omega)$ at all ω. This increase in L also causes the terminal frequency of $G^*_{tens}(\omega)$ to drop into the range of frequencies shown, allowing $G^*(\omega)$ to approach its high-frequency asymptote of $G^* \propto (i\omega)^{3/4}$ for $\omega \gtrsim 10^2$–10^3 rad/s in Figure 5b,c. The system with $L = 10L_p$ is also beginning to form an intermediate frequency regime, visible in Figure 5c at $\omega \sim 10^1$–10^2 s^{-1}, in which $G^*_{tens}(\omega) \sim (i\omega)^{1/2}$, due to the diffusion of excess length along a coil-like tube contour, as predicted for $L \gg L_p$.

The moduli plotted in Figures 5–7 do not include the solvent contribution to $G''(\omega)$ of $G''_{solvent}(\omega) = i\omega\eta_s$. Inclusion of such a contribution, with a viscosity $\eta_s = 0.01$ Poise, would have little visible effect upon the plots shown in Figures 5–7, in the range of frequencies shown but would become significant in this frequency range for slightly lower polymer concentrations or slightly shorter chains. Because the solvent contribution to $G''(\omega)$ increases linearly with ω, while the polymer contribution increases as $\omega^{3/4}$, the solvent contribution will always dominate at sufficiently high frequencies.

In section V, we consider rheological studies of very polydisperse solutions of *F*-actin filaments. To take into account the effects of polydispersity, we take

$$G(t) = \int_0^\infty dL\ \rho(L)\ G(t; L) \qquad (127)$$

where $G(t; L)$ is the calculated contribution to $G(t)$ per unit chain length of chains with length L, calculated using fixed values of L_e and q_e, and where $\rho(L)\ dL$ is the density of contour length per unit volume due to chains with lengths between L and $L + dL$. This expression follows from the physical assumption that, in a step deformation, all chains undergo the same initial strain and yield independent contributions to the stress. Results for a polydisperse solution with an exponential distribution of chain lengths, with $\rho(L) = (\rho L/\bar{L}^2)e^{-L/\bar{L}}$ and $\bar{L} = L_p = 17\ \mu$m, are given in Figure 6.

D. Effects of Cross-Links. It is interesting to briefly compare the behavior predicted above for solutions to that expected for a physically or chemically cross-linked gel of wormlike chains. In a gel, the presence of a cross-link between any two chains is expected to prevent the tangential motion of each chain along its own tube. Since this tangential motion is required for the redis-

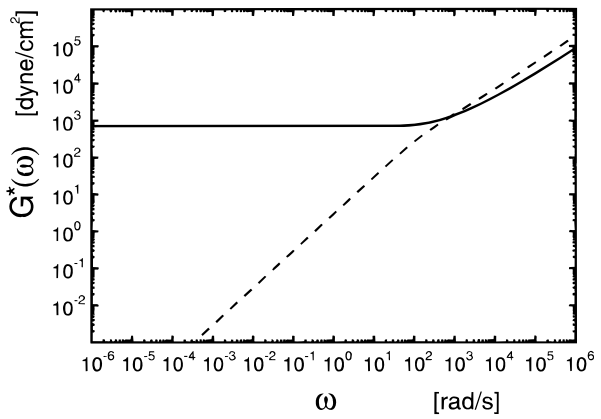

Figure 7. Values of $G'(\omega)$ and $G''(\omega)$ for a system with $G^*(\omega) = {}^1/_{15}\rho\hat{B}(\omega)$, which is an approximation to the behavior of a lightly cross-linked gel, for the set of parameters used in Figures 5 and 6.

tribution of excess length, the presence of cross-links is expected to partly or fully suppress the otherwise rapid relaxation of tension following a step deformation. The presence of even a relatively low density of cross-links can thus drastically effect the low-frequency behavior of $G^*(\omega)$, leading to a situation in which $G^*(\omega)$ is dominated by the appearance of a broad elastic plateau in $G'_{\text{tens}}(\omega)$, with a plateau modulus that can be orders of magnitude larger than that predicted for fully mobile chains.

A simplified model for the modulus $G^*(\omega)$ of a gel is most easily obtained for the case in which the average distance between cross-links on a single chain remains as follows: (i) less than L, so that there are few dangling ends, (ii) less than L_p, so that the subchains between cross-links remain relatively straight and so that the tension induced in each segment by a step deformation is relatively uniform and cannot be significantly relaxed by redistribution of excess length within a subchain, but (iii) longer than L_e, so that the low-frequency limit of the effective single-chain extension modulus $\hat{B}(\omega)$ is still controlled by L_e rather than by the distance between cross-links. In this regime the cross-links act only to suppress the relaxation of tension, yielding $\psi^*(\omega)=1$ in eq 103, without significantly changing the modulus $\hat{B}(\omega)$, thus yielding a modulus $G^*_{\text{tens}}(\omega) = {}^1/_{15}\rho\hat{B}(\omega)$. The resulting approximation for $G^*_{\text{tens}}(\omega)$, which is shown in Figure 7, exhibits a plateau modulus that, for the set of parameters used here, is about 700 times larger than that predicted for the corresponding un-cross-linked solution, in which $G' \sim G_{\text{curve}}(0)$. This approximation for the plateau modulus is identical to one proposed by MacKintosh et al.[37]

In the simplified model defined above, we have assumed that the relaxation of tension is completely suppressed for all parts of all chains in the system. In fact, only segments of chain that are trapped between two permanent cross-links can contribute to the zero-frequency modulus, because a nonzero tension can persist indefinitely only in these "elastically active" chain segments and not in the remaining dangling ends and un-cross-linked chains. To describe very lightly cross-linked systems, the above approximation should thus, at a minimum, be corrected by replacing the total contour length density ρ by the corresponding density of elastically active chain length when estimating the plateau modulus. For the parameters used above, however, we would still obtain a plateau modulus an order of magnitude higher than $G_{\text{curve}}(0)$ if the density of elastically active strands was only 1.5% of the total.

IV. Optical Response

We now consider the linear response of the optical refractive index $\mathbf{n}(t)$, which is described by the response function $\mu(t)$ defined in eq 7.

The initial value of $\mu(t)$ obtained immediately after a step deformation is calculated in Appendix A, where we obtain

$$\mu(0) = \frac{4 + \bar{g}}{5}\rho A \tag{128}$$

Here $\bar{g}$ is a function $\bar{g}(\beta) = 2(1 - \beta - e^{-\beta})/\beta^2$ of the ratio $\beta = 3L/L_p$, with limiting values $\bar{g}(0) = -1$ and $\bar{g}(\infty) = 0$. Like g_{end} in eq 58, the function $\bar{g}(\beta)$ takes into account the effects of tangential flow of the polymer during a step deformation. The instantaneous value $\mu(0)$ is simply proportional to ρ and (aside from the weak dependence of $\bar{g}$ on the ratio L/L_p) is nearly independent of L and L_p.

A formal expression for the time dependence of $\mu(t)$ at times $t \gg \tau_e$, where the primitive chain model applies, may be obtained by reasoning similar to that used to calculate $G_{\text{orient}}(t)$. We write

$$\mathbf{n}(t) = A\int d\mathbf{u}\,(\mathbf{uu} - {}^1/_3\boldsymbol{\delta})\bar{f}(\mathbf{u},t) \tag{129}$$

where $\bar{f}(\mathbf{u},t)$ is the average of $f(\mathbf{u},s,t)$ over the length of the chain, and note that, because $\mathbf{n}(t)$ is expressed as the angular integral of an irreducible second rank tensor, it must decay as

$$\mu(t) = \mu(0)\bar{\chi}_2(t) \tag{130}$$

where $\bar{\chi}_l(t)$ is the decay function for the $l = 2$ spherical harmonic components of $\bar{f}(\mathbf{u},t)$. A series expression for $\bar{\chi}_l(t)$ may be obtained from series 67, which yields

$$\bar{\chi}_2(t) = \sum_{k=1}^{\infty} \frac{8}{q_{2k}L}\frac{\sin^2(q_{2k}L/2)}{q_{2k}L + \sin(q_{2k}L)}e^{-D_{\text{rep}}q_{2k}^2 t} \tag{131}$$

Below, we discuss the limiting behaviors obtained for coil-like and rod-like chains.

In the limit $L \gg L_p$ of coil-like chains, the function $\bar{\chi}_2(t)$ exhibits two time regimes: At times $t \lesssim \tau_{\text{end}}$, the end of the chain retains a signficant degree of anisotropy, the value of $\chi_2(s,t)$ at the end of the chain remains of order unity, and $\bar{\chi}_2(t)$ remains very close to unity. At times $t \gg \tau_{\text{end}}$, when the orientations of the ends of the chain have been randomized and $\chi_2(s,t)$ nearly vanishes at either end of the chain, the subsequent time dependence of $\chi_2(s,t)$ may be approximated by replacing boundary condition 66 by an absorbing boundary condition at each chain end. This yields a time dependence for $\bar{\chi}_2(s,t)$ that is nearly identical to that of the DE response function $\chi(s,t)$, which is obtained from the solution of diffusion equation 47 with absorbing boundary conditions. In the limit of long chains, we thus find $\bar{\chi}_2(t) \simeq 1$ for $t \lesssim \tau_{\text{end}}$ and

$$\lim_{L \gg L_p} \chi_2(t) \simeq \bar{\chi}(t) \tag{132}$$

at all times $t \gg \tau_{\text{end}}$.

In the limit of rod-like chains, the relaxation of $\bar{\chi}_2(t)$ is controlled by the diffusive randomization of the overall chain orientation, which was described in our calculation of $G_{orient}(t)$ and which yields a simple exponential decay

$$\lim_{L \ll L_p} \bar{\chi}_2(t) \simeq e^{-t/\tau_{rod}} \tag{133}$$

with the same decay time as that appearing in $G_{orient}(t)$.

In both limits, the function $\mu'(\omega)$ is thus found to to exhibit a single plateau, with a plateau value given by $\mu(0)$ and a characteristic relaxation time given by the longest relaxation time found in $G(t)$, i.e., a relaxation time τ_{rep} when $L \gg L_p$ and τ_{rod} when $L \ll L_p$. Unlike $G^*(\omega)$, $\mu^*(\omega)$ is not expected to exhibit either a second plateau or a power law regime at frequencies greater than τ_e^{-1}, since the more complicated high-frequency behavior of $G^*(\omega)$ is controlled by the relaxation of tension, which in the tightly-entangled regime has essentially no effect upon the distribution of segment orientations and thus no effect upon the optical birefrigence.

V. *F*-Actin Solutions

The systems that best satisfy the requirements for the validity of the model developed in section IV are probably entangled solutions of extremely long, stiff biopolymers, including semiflexible protein filaments such as actin. Below, we make some preliminary comparisons of the predictions of the above model to existing data on the linear viscoelastic response of *F*-actin solutions.

Actin forms a helical protein filament of 70−80 Å in diameter, which contains a helical repeat unit of 360 Å, containing 13 protein monomers, each of a molecular weight of about 43 000.[22] The persistence length has been measured by several groups by analyzing the Brownian fluctuations of flourescently labeled chains,[23,24] giving $L_p \simeq 17\ \mu$m. Measurements of the distribution of chain lengths produced by typical polymerization protocols indicate the existence of a broad, approximately exponential distribution, with reported average chain lengths (in the absence of capping proteins) of $\bar{L} \simeq 5-25\ \mu$m. The experiments discussed here have used solutions with actin concentrations, denoted by c_A, of $c_A = 0.05-2.5$ mg/mL, giving actin volume fractions of signficantly less than 1%. A solution with $c_A = 1$ mg/mL has a contour length concentration $\rho = 39\ \mu m^{-2}$, yielding a mesh size $\rho^{-1/2} \simeq 0.16\ \mu$m that is less than L_p by a factor of 100. Such solutions are observed[20] to begin forming nematic domains at concentrations above $\rho_{nem} \simeq 2.5$ mg/mL.

Experiments by Käs and co-workers,[19,20] in which flourescently labeled actin are visualized by optical microscopy, have confirmed that, at these concentrations, each actin filament is confined to a tube of diameter comparable to the mesh size and that the filaments move primarily by reptation. Such experiments yield optically determined tube diameters of 0.1−1.0 μm, which are found to vary with changes in c_A as $D_e \propto c_A^{-0.5\pm0.15}$. By taking many micrographs of each polymer as it fluctuates within the tube, overlaying the images, and measuring the width of the region enclosed by the resulting tangle of lines, Käs et al. obtain a tube diameter of approximately 0.4 μm for $c_A = 1$ mg/mL, which we estimate[52] corresponds to a value $D_e \simeq 0.2\ \mu$m for the tube diameter defined in eq I.39.

Figures 5 and 6 show theoretical results for monodisperse and polydisperse solutions with a concentration $c_A = 1$ mg/mL, calculated using the parameters discussed above. Corresponding values for other concentrations have been obtained by assuming that $D_e \propto c_A^{-3/5}$ and $L_e \propto c_A^{-2/5}$.

A. Mechanical Rheometry. Over the past decade, several experimental groups[2−5,7−12,14−16] have reported measurements of $G^*(\omega)$ by conventional mechanical rheometry, which collectively span a frequency range of $\omega = 10^{-4}-10^2$ rad/s. All authors have reported the existence of a single plateau in $G'(\omega)$, but there has been ongoing disagreement about even the order of magnitude of the plateau modulus. The inability of different groups to reproduce each others' results, which is thus far assumed to be the result of slight differences in sample preparation, make it difficult for us to draw any firm conclusions regarding the agreement of theory and experiment, though the theory does suggest one possible source of such discrepancies. The results obtained thus far may be summarized as follows:

Measurements by Sackmann and co-workers in Munich[10−12] yield results that are consistent with a plateau modulus of $G' \simeq 1-2$ dyn/cm^2 for $c_A = 1$ mg/mL, which is very close to the value of $G' \simeq 1$ dyn/cm^2 predicted above, and show a concentration dependence of $G' \propto c_A^{1.4}$,[12] as predicted for a curvature dominated plateau. There are, however, signficant discrepancies between theoretical predictions and the results of refs 10 and 11 for the frequency dependence of $G^*(\omega)$: The storage modulus $G'(\omega)$ reported in refs 10 and 11 exhibits a plateau that extends only up to frequencies of order 10^{-1} rad/s, and instead increases approximately as $G'(\omega) \propto \omega^{1/2}$ for $\omega \simeq 10^{-1}-10^1$ rad/s,[10] while the plateau in the calculated storage modulus is broader and extends to about 10 rad/s. More recent results[12,53] from this group show a broader plateau, in better agreement with the predicted behavior. Only the data from this group shows an apparent terminal frequency within the experimentally accessible window.

Rheological measurements by Pollard, Schwarz, and co-workers[2−5] and more recent measurements by Xu et al.,[14−16] all at Johns Hopkins University, yield a much broader plateau with reported plateau moduli spread throughout the range 2−20 dyn/cm^2 for samples with $c_A \simeq 1$ mg/mL. Xu et al.[15] report that the storage moduli of a series of samples with different concentrations, measured at a fixed frequency of 1 rad/s, vary with concentration as $G' \propto c_A^{1.2\pm0.2}$, consistent with prediction of $G' \propto c_A^{1.4}$, though the reported modulus of $G' \simeq 14$ dyn/cm^2 for the sample with 1 mg/mL is significantly larger than our theoretical estimate of 1 dyn/cm^2. In all the data reported from Johns Hopkins, $G'(\omega)$ remains signficantly larger than $G''(\omega)$ at the lowest accessible frequency of 10^{-3} rad/s, suggesting a very low terminal relaxation frequency.

Measurements by Janmey and co-workers in Boston[6−9] have, until recently,[16] consistently reported signficantly higher, and variable, values of the plateau modulus, typically giving moduli of $G' \sim 10^2-10^4$ dyn/cm^2 at concentrations on the order of 1 mg/mL. In ref 8, these authors fit data for the plateau modulus from 8 different concentrations to a power law $G' \propto \rho^{2.2}$, with a fitted

value of $G' \sim 100$ dyn/cm^2 at 1 mg/mL. Recent measurements of the plateau modulus using a torsional pendulum by Böhm and Käs[21] also give a value of $G' \simeq 170$ dyn/cm^2 at $c_A \simeq 1.0$ mg/mL, which are also found to vary as $c_A^{2.14\pm0.2}$ for a set of four samples with concentrations $c_A = 0.25-1.5$ mg/mL. The simultaneous existence of such large values of the plateau modulus (2−3 orders of magnitude larger than those predicted for a curvature-dominated plateau) and long relaxation times (at least 3 orders of magnitude longer than those predicted for the relaxation of tension) cannot be explained by the model developed here, which assumes relatively free tangential motion. Both the absolute magnitudes and the concentration dependence of the plateau modulus found in these experiments seem to instead be consistent with those expected for a lightly cross-linked gel, as discussed above, to which the model of MacKintosh et al.[37] (which was motivated by these data) should apply.

A recent collaboration of the Johns Hopkins and Harvard[16] groups showed that a modulus of roughly 5 dyn/cm^2 for $c_A = 1$ mg/mL could be reproducibly obtained from freshly polymerized *F*-actin[54] and documented the surprising sensitivity of the modulus to differences in polymerization and, particularly, storage conditions. The values obtained for the plateau modulus in this study are, however, still about a factor of 5 larger than the values reported by the Munich group, which are in quantitative agreement with the estimate obtained above by using Käs et al.'s measurement of D_e to estimate L_e. The theory suggests the possibility that the sensitivity to preparation conditions could be a consequence of the development of very small amounts of cross-linking in some samples. This is consistent with the observation that the lowest measured values of the plateau modulus are closest to our estimate.

B. Microrheometry. Several groups have also published results of microrheological measurements in which the properties of an actin solution are deduced from observations of either the forced[13,17] or Brownian[15,17,18] motion of small spheres embedded in the fluid. Recent experiments by Amblard et al.,[17] Gittes et al.,[18] Xu et al.,[15] and Gissler and Weitz,[55] which use various light scattering techniques to measure bead displacements, have extended the accessible frequency range up to $\omega \simeq 10^4-10^5$ rad/s. All of these authors have reported results consistent with the existence of a complex modulus that varies as $G^*(\omega) \propto (i\omega)^{3/4}$ at frequencies $\omega \gtrsim 100$ rad/s, in striking agreement with our prediction for the frequency dependence of $G^*(\omega)$ at high frequencies.

In order to also compare predicted and measured values of absolute magnitudes of the modulus in this power law regime, a quantitative comparison has been made to the results of Gittes et al.[18] in Michigan. This group has used laser interferometry to directly measure the spectral density $\langle|x(\omega)|^2\rangle$ of the bead displacement over a frequency range of $\omega \simeq 10^{-1}-10^5$ rad/s, where $x(\omega) \equiv \int dt\, e^{-i\omega t}\, x(t)$ and $x(t)$ is the displacement of the bead along a single Cartesian direction. Gittes et al.[18] show by a straightforward application of the fluctuation−dissipation theorem that if the medium surrounding a bead may be described as a single-component, spatially homogeneous, incompressible, viscoelastic fluid with a no-slip boundary condition at the bead surface, then the spectral density of the bead displacement[56] is

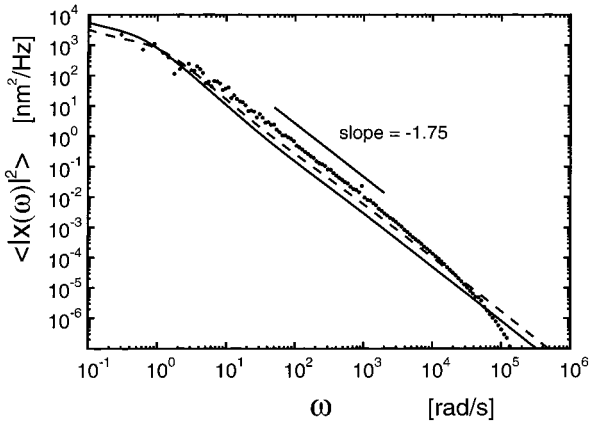

Figure 8. Predicted power spectral density $\langle|x(\omega)|^2\rangle$ for the displacement of a bead of diameter $2R = 5.0$ μm in an actin solution of concentration $c_A = 1$ mg/mL, with an exponential distribution of chain with $L = 17$ μm, calculated for assumed persistence lengths of $L_p = 17$ μm (solid line) and $L_p = 9$ μm (dashed line), compared to the optical measurements of Schnurr and Gittes et al. (dots) for a sample with these values of c_A and R. This data set was originally presented in Figure 7D of ref 18 and is reproduced here by courtesy of the authors. The calculated spectral densities are somewhat sensitive to the assumed chain length distribution at frequencies $\omega \lesssim 10^3$ rad/s, which is not well characterized, and can deviate noticeably from a pure power law behavior at these frequencies. The decrease in the slope of the experimental values of $\langle|x(\omega)|^2\rangle$ at $\omega \gtrsim 10^4$ rad/s is believed by the authors of ref 18 to be an experimental artifact, of unknown origin, since it is reportedly also observed for beads in pure solvent.

given rigorously by

$$\langle|x(\omega)|^2\rangle \simeq \frac{1}{3\pi R\omega} Im\left(\frac{1}{G^*(\omega)}\right) \qquad (134)$$

where $Im(...)$ denotes an imaginary part, R is the bead radius, and $G^*(\omega)$ is the complex modulus of the surrounding fluid. Measurements taken with the largest beads, of diameter 5.0 μm, yield a power spectrum that varies as $\langle|x(\omega)|^2\rangle \propto \omega^{-1.75}$ over a frequency range of $\omega \simeq 1-10^4$ rad/s as shown in Figure 8. By numerically applying the Kramers−Krönig relation to the measured power spectra, the authors then infer a complex modulus that varies as $G^*(\omega) \propto (i\omega)^{0.75}$. The fact that the power law regime in the power spectrum extends to such low frequencies, with no clear sign of a plateau, suggests that the samples used by this group have plateau moduli of a few dyn/cm^2 or less at $\omega \simeq 0.1$ rad/s.

To compare theoretical predictions to these measurements, we have used calculated values of $G^*(\omega)$ in eq 134 to obtain theoretical predictions for the spectral density, thus inverting the experimental analysis. By comparing spectral densities, rather than moduli, we may bypass any uncertainties arising from the use of the Kramers−Krönig relation to invert experimental data taken over a finite range of frequencies. In Figure 8, we compare calculated and measured spectra for a polydisperse 1 mg/mL solution. The calculated spectra, like the data, exhibit an apparent power law with a slope of close to −1.75 down to frequencies of about 1 rad/s. The absolute magnitude of the calculated spectral density for $L_p = 17$ μm is, however, found to be about 4 times smaller than the measured value, as indicated in Figure 8. Correspondingly, the calculated moduli are roughly 4 times larger than those inferred from these data.

One possible reason for this quantitative discrepancy is (we now argue) that there exists a significant depletion of polymer through a region surrounding each bead, which is not accounted for in the analysis leading to eq 134. Because the measured persistence length of $L_p = 17\ \mu$m is over 3 times the largest bead diameter of 5 μm, the chains interact with the beads almost as rigid rods and must for geometrical reasons be largely excluded from a corona with a thickness on the order of the bead radius around each bead. If we idealize the chains as infinite rigid rods, the contour density $\rho(r)$ of polymer at a distance r from the center of a bead of radius R may be obtained by considering the range of rod orientations blocked by the presence of the bead, giving $\rho(r) \simeq \rho[r^2 - R^2]^{1/2}/r$, where ρ is the bulk density of polymer. This depletion of polymer near each bead is expected to result in a substantial decrease in the viscoelastic restoring forces opposing motion of the bead, and a corresponding increase in the magnitude of Brownian fluctuations.

Another possible source of this discrepancy is a possible error in the value of the persistence length, $L_p = 17\ \mu$m, thus far assumed in our analysis. A fluorescence microscopy study by Isambert et al.[57] yielded a persistence length of $18 \pm 1\ \mu$m for actin filaments that are stabilized by fluorescently labeled phalloidin, in agreement with the two earlier experiments on such phalloidin-stabilized filaments,[23,24] but yielded a smaller persistence length of $9 \pm 0.5\ \mu$m for actin filaments that are not a stabilized by phalloidin, such as those used in this and other rheological measurements. Use of the smaller value of $L_p = 9\ \mu$m lowers the absolute value of $G^*(\omega)$ at high frequencies by about a factor of 2 (see eq 35), thus decreasing the discrepancy between theory and experiment to roughly a factor of 2, as shown by the dashed line in Figure 8, while having little effect upon our estimate of the plateau modulus, which depends more weakly upon L_p.

In light of the uncertainties in the experimental analysis caused by the expected depletion of actin near a bead, the remaining uncertainty in the value of L_p, and other remaining experimental uncertainties, the predicted absolute value of $G^*(\omega)$ is judged to be in reasonable quantitative agreement with experiment.

VI. Summary

This paper presents a calculation of the linear viscoelastic response of a solution of tightly-entangled semiflexible chains within the context of the tube model. The model and results are analogous in many ways to those obtained in the DE tube model of flexible chains: For chains of length $L \simeq L_p$, we find a broad elastic plateau in $G^*(\omega)$ whose magnitude is controlled here by a curvature contribution that is the closest analog of the entropic elastic stress of a solution of flexible chains, while at higher frequency we find a power law behavior that is characteristic of the viscoelastic response of unentangled wormlike chains, which is the closest analog of the Rouse-like behavior seen at high frequencies in systems of flexible chains. One important distinction between this model and the tube model of flexible chains is that, in solutions of semiflexible chains, we expect a separation of free energy scales between curvature stress contributions arising from forces (including Brownian forces) that act perpendicular to the polymer, which are predicted to dominate the low-frequency plateau, and tension contributions arising from forces that act parallel to the chain, which are predicted to dominate the high-frequency power law regime.

One consequence of the disparity between the free energy scales of the curvature and tension contributions to the modulus is that the value of the plateau modulus is found to be extremely sensitive to the presence of anything that hinders tangential motion of the polymer along the tube, such as permanent or long-lived cross-links between polymers. By preventing the otherwise rapid relaxation of tension to the ends of the chain, such cross-links can cause the formation of a low-frequency elastic plateau in $G^*_{tens}(\omega)$ with a plateau modulus orders of magnitude larger than that predicted for the un-cross-linked solution. This stands in contrast to the behavior observed in entangled solution and melts of flexible polymers, in which the addition of a small density of cross-links has little effect upon the plateau modulus and acts only to suppress the terminal relaxation rate to zero.

The limitations of the model are primarily determined by the limitations of the physical assumptions outlined in section I. The most important mathematical approximation that has been added to these physical assumptions is our use of a harmonic potential to mimic the confinement of the polymer to a tube, which introduces some uncertainty into our attempts to predict the plateau modulus from knowledge of the measured tube diameter, but which is expected to be a substantial improvement over dimensional analysis alone. The only parameters in the resulting model are the persistence length L_p and contour lengths L of the chains, the friction coefficients ζ and $\zeta_\perp$, and the tube diameter D_e.

As a first application, the predictions of the model have been compared to the results of recent experiments on *F*-actin solutions, for which the persistence length and tube diameters have been measured by fluorescence microscopy, allowing us to make a parameter-free comparison of theoretical predictions to the results of rheological measurements.

Attempts to compare theoretical predictions for the plateau modulus to the results of mechanical rheometry measurements are complicated by the fact that there have been large discrepancies between the plateau moduli reported by different experimental groups. Our estimate of the absolute magnitudes and concentration dependence for the plateau modulus is found to agree quite well with the results of Sackmann's group in Munich. The moduli measured by Pollard, Schwarz, Xu, Wirtz, and co-workers in Baltimore vary from 2 to 15 times our theoretical estimate. Plateau moduli reported by Janmey and co-workers in Boston, which have until recently been 10−1000 times larger than those measured by others, are much too large to be explained as consequences of curvature stress and instead exhibit both absolute magnitudes and a concentration dependence consistent with those expected for the tension-dominated plateau modulus of a lightly cross-linked gel. We will show in the following paper in this series[58] that the nonlinear rheological behavior found in these high-modulus samples is also inconsistent with that expected for a solution of tangentially mobile chains but consistent with that expected for a gel.

Theoretical predictions for the high-frequency behavior of $G^*(\omega)$ are found to be in satisfactory quantitative agreement with the results of recent microrheometry experiments. The predicted frequency dependence of

$G^*(\omega) \propto (i\omega)^{3/4}$ is in excellent agreement with that found in several recent microrheometry studies. The predicted absolute magnitude of $G^*(\omega)$ in this power law regime (which contains no adjustable parameters) is 2−4 times greater than that inferred from the experiments of the Michigan group,[18] which is arguably within the combined uncertainties of the experiment and the analysis required to infer a modulus from such an optical measurement.

It would be particularly useful for future experimental work to systematically search for evidence of crossovers between the different concentration regimes proposed for isotropic solutions of semiflexible polymers and to test the applicability of the model to tightly-entangled model systems other than *F*-actin, with more easily reproducible physical properties, if such can be found.

Acknowledgment. I would like to acknowledge helpful conversations with Fred MacKintosh, Tony Maggs, Denis Wirtz, Fred Gittes, Tom Mason, Jingyuan Xu, Thomas Gissler, and Dave Weitz and the partial financial support of the Exxon Education Foudation.

Appendix A: Equilibrium Statistics

We first review the use of a diffusion equation to describe the equilibrium distribution of conformations of a wormlike chain. The quantity of interest here is the conditional probability $D(\mathbf{u}',s';\mathbf{u},s'')$ that $\mathbf{u}(s') = \mathbf{u}'$ given that $\mathbf{u}(s'') = \mathbf{u}''$, which describes correlations of $\mathbf{u}$ along the chain. This quantity can be expressed as a function $D(\mathbf{u}',\mathbf{u}'',S)$, where $S \equiv |s' - s''|$. For $S \neq 0$, D obeys a rotational diffusion equation

$$\left[\frac{\partial}{\partial S} - D_{\mathrm{eq}}\frac{\partial^2}{\partial \mathbf{u}^2}\right] D\,(\mathbf{u},\mathbf{u}',S) = 0 \qquad \text{(A1)}$$

with an initial condition $D(\mathbf{u},\mathbf{u}',0) = \delta^{(2)}(\mathbf{u} - \mathbf{u}')$ and an effective diffusivity $D_{\mathrm{eq}} \equiv 1/(2L_{\mathrm{p}})$. Expanding D in spherical harmonics yields

$$D\,(\mathbf{u},\mathbf{u}',S) = \sum_{lm} Y_{lm}(\mathbf{u})\; Y^*_{lm}(\mathbf{u}')\; \mathrm{e}^{-l(l+1)D_{\mathrm{eq}}S} \qquad \text{(A2)}$$

We may use the above, together with the fact that the correlations of the vector $\mathbf{u}(s)$ and the traceless symmetric tensor $\mathbf{S}(s) \equiv \mathbf{u}(s)\mathbf{u}(s) - {}^1/_3\boldsymbol{\delta}$ are controlled by, respectively, the $l = 1$ and $l = 2$ components of $D(\mathbf{u},\mathbf{u}',S)$, in order to show that

$$\langle u_i(s)\; u_j(s')\rangle_{\mathrm{eq}} = {}^1/_3\delta_{ij}\; \mathrm{e}^{-|s-s'|/L_{\mathrm{p}}} \qquad \text{(A3)}$$

$$\langle S_{ij}(s)\; S_{kl}(s')\rangle_{\mathrm{eq}} = {}^1/_{15}P_{ijkl}\; \mathrm{e}^{-3|s-s'|/L_{\mathrm{p}}} \qquad \text{(A4)}$$

where $P_{ijkl} \equiv \delta_{ik}\delta_{jl} + \delta_{il}\delta_{jk} - {}^2/_3\delta_{ij}\delta_{kl}$.

The above description of correlations in the equilibrium state may be used to derive boundary condition 50 for the diffusion equation of $f(\mathbf{u},s,t)$. Reptation may be described by a stochastic process involving periodic discrete jumps of the chain by a random amount Δs once every time Δt, such that

$$\mathbf{u}(s,t+\Delta t) = \mathbf{u}(s+\Delta s,t) \qquad \text{(A5)}$$

for points far from either end of the chain. If $\Delta s > 0$ for the time interval between t and $t + \Delta t$, then there exists a segment near the $s = L$ end of the chain which spans coordinates $L - \Delta s < s < L$ at time t, whose conformation at time $t + \Delta t$ must instead be chosen randomly from an equilibrium distribution of conformations for a chain segment of length Δs for which one end is constrained to take on an orientation $\mathbf{u}(L,t)$. A similar process, involving the creation of a new segment of tube at the $s = 0$ end of the chain, applies when $\Delta s < 0$.

The resulting creation of new chain segments at either end of the chain can also be described by stochastic process A5 if we define the function $\mathbf{u}(s)$ for each chain in our statistical ensemble to extend beyond the physical domain $0 < s < L$ and require that the conformations of the added fictitious portions of the chain are always thermally equilibrated, i.e., that the conformations of the chain for $s > L$ and $s < 0$ be chosen randomly from the equilibrium distribution of chain conformations, subject to the constraint that $\mathbf{u}(s)$ must remain continuous at $s = 0$ and $s = L$ for each chain in the ensemble. We may make this notion precise by defining

$$f(\mathbf{u},s,t) = \int \mathrm{d}\mathbf{u}'\; D\;(\mathbf{u},s;\mathbf{u}',L)\; f\;(\mathbf{u}',L,t) \qquad \text{(A6)}$$

for $s > L$, and by an analogous definition for $s < 0$. Boundary condition 50 then follows immediately from the requirement that $\partial f/\partial s$ remains continuous at $s = 0$ and $s = L$.

Appendix B: Motion of a Single Chain

Here, we give a statistical description of the motion of a single nearly-inextensible wormlike primitive chain within a homogeneously deforming, tightly-entangled solution. We proceed in two steps: We first consider the relatively slow relaxation of the distribution of conformations of the primitive chain via reptation, while treating the chain for this purpose as inextensible. We then take into account the effects of the slight extensibility of the chain and the resulting rapid diffusion of excess length.

A. Reptation. We consider a polymer within a flow described by a macroscopic fluid velocity $\mathbf{v}(r,t)$ at point $\mathbf{r}$ and time t, with a spatially homogeneous rate-of-deformation tensor $\boldsymbol{\kappa}^\dagger(t) = \nabla\mathbf{v}$, so that $\mathbf{v}(\mathbf{r},t) = \mathbf{v}(0,t) + \boldsymbol{\kappa}(t)\cdot\mathbf{r}$. The velocity of a point s along the primitive chain is given (in a continous representation of the chain) by a sum

$$\partial\mathbf{r}(s)/\partial t = \boldsymbol{\kappa}\cdot\mathbf{r}(s) + \nu(s)\;\mathbf{u}(s) \qquad \text{(B1)}$$

of a velocity component $\boldsymbol{\kappa}\cdot\mathbf{r}(s)$ that follows the macroscopic flow field plus a tangential velocity $\nu(s)$ of the polymer along its own local tangent vector. The tangential velocity ν may be expressed as a sum

$$\nu(s,t) = \bar{\nu}(s,t) + \Delta\nu(t) \qquad \text{(B2)}$$

of a random component $\Delta\nu(t)$ that gives rise to the one-dimensional Brownian motion (i.e., reptation) of the chain along its contour and an average velocity $\bar{\nu}(s,t)$. The random component $\Delta\nu(t)$ is independent of s and has white-noise temporal correlations

$$\overline{\Delta\nu(t)\;\Delta\nu(t')} = 2D_{\mathrm{rep}}\delta(t - t'), \quad \overline{\Delta\nu(t)} = 0 \qquad \text{(B3)}$$

The overbar in eqs B2 and B3 denotes an average over Brownian fluctuations of $\nu(s)$ but not over chain conformations.

As in (I), we describe the chain by a local tangent vector $\mathbf{u}(s) \equiv \partial\mathbf{r}/\partial s$ and a curvature $\mathbf{w}(s) \equiv \partial\mathbf{u}/\partial s$. The intensibility is imposed by requiring that $|\mathbf{u}(s,t)| = 1$ for all s and t. Equations of motion for $\mathbf{u}(s)$ and $\mathbf{w}(s)$ may be obtained by differentiating eq B1 with respect to s. Differentiating once yields

$$\frac{\partial \mathbf{u}(s)}{\partial t} = \mathbf{g}(\mathbf{u}(s)) + \nu(s)\frac{\partial \mathbf{u}(s)}{\partial s}$$

$$\mathbf{g}(\mathbf{u}) \equiv (\boldsymbol{\delta} - \mathbf{uu})\cdot\boldsymbol{\kappa}\cdot\mathbf{u} \qquad \text{(B4)}$$

where $\nu(s)$ must satisfy an auxiliary constraint

$$\partial\bar{\nu}(s)/\partial s = -\boldsymbol{\kappa}:\mathbf{u}(s)\,\mathbf{u}(s) \qquad \text{(B5)}$$

necessary to impose the requirement that $\partial|\mathbf{u}(s,t)|^2/\partial t = 0$. Differentiating again with respect to s, while again applying constraint B5, yields

$$\frac{\partial \mathbf{w}(s)}{\partial t} = \mathbf{G}(\mathbf{u}(s))\cdot\mathbf{w}(s) + \nu(s)\frac{\partial \mathbf{w}(s)}{\partial s}$$

$$\mathbf{G}(\mathbf{u}) \equiv \boldsymbol{\kappa} - 2\boldsymbol{\delta}(\boldsymbol{\kappa}:\mathbf{uu}) - \mathbf{u}\,(\boldsymbol{\kappa} + \boldsymbol{\kappa}^\dagger)\cdot\mathbf{u} \qquad \text{(B6)}$$

where $\mathbf{G}(\mathbf{u})$ is a second-order tensor. It is straightforward to confirm that eqs B4 and B6 automatically preserve the requirement that $|\mathbf{u}(s)|^2 = 1$ and that $\mathbf{u}(s)\cdot\mathbf{w}(s) = 0$ for all s and t.

We now derive Fokker−Planck equations for the probability distributions defined in eqs 44 and 45. Differentiating these definitions with respect to t, while using eqs B4 and B6 for $\partial\mathbf{u}/\partial t$ and $\partial\mathbf{w}/\partial t$, and averaging over fluctuations of $\Delta\nu$, yields

$$\left[\frac{\partial}{\partial t} - D_{\mathrm{rep}}\frac{\partial^2}{\partial s^2}\right]f = -\frac{\partial}{\partial \mathbf{u}}\cdot(\mathbf{g}f) + \left\langle \bar{\nu}\frac{\partial \hat{f}}{\partial s}\right\rangle \qquad \text{(B7)}$$

$$\left[\frac{\partial}{\partial t} - D_{\mathrm{rep}}\frac{\partial^2}{\partial s^2}\right]\mathbf{F} = -\frac{\partial}{\partial \mathbf{u}}\cdot(\mathbf{gF}) + \mathbf{G}\cdot\mathbf{F}^\dagger + \mathbf{F}\cdot\mathbf{G}^\dagger + \left\langle \bar{\nu}\frac{\partial}{\partial s}(\mathbf{w}\mathbf{w}\hat{f})\right\rangle \qquad \text{(B8)}$$

where $f = f(\mathbf{u},s)$, $\mathbf{F} = \mathbf{F}(\mathbf{u},s)$, $\bar{\nu} = \bar{\nu}(s)$, and $\hat{f} = \hat{f}(\mathbf{u},s)$, and where $\partial/\partial\mathbf{u}$ is the gradient operator on the unit sphere, which has nonzero components only in the two directions perpendicular to $\mathbf{u}$. In the above, the action of the diffusion operator on the left hand side represents the effects of 1D Brownian motion along the contour of the chain, while the terms on the right hand side describe the effects of the flow. The last terms in eqs B7 and B8, in angle brackets, describe the convection of probability by the average tangential velocity $\bar{\nu}(s)$.

To describe the response of the system to a continuous flow field, or the initial response to a step deformation, we will need an explicit expression for the tangential velocity $\bar{\nu}(s)$. An explicit expressions for the tangential velocity of an inextensible chain of specified conformation may be constructed by combining eq B5 for $\partial\nu/\partial s$, which is a consequence of inextensibility, with eq 18, which relates $\bar{\nu}(s)$ and $\mathscr{T}$. This yields a differential equation

$$\partial^2\mathscr{T}(s)/\partial s^2 = -\zeta\mathbf{u}(s)\,\mathbf{u}(s):\boldsymbol{\kappa} \qquad \text{(B9)}$$

for $\mathscr{T}(s)$, for which we require that $\mathscr{T}(0) = \mathscr{T}(L) = 0$. The solutions of eqs B9 and 18 may be expressed as integrals

$$\mathscr{T}(s) = \zeta\int_0^L \mathrm{d}s'\, K(s,s')\,\mathbf{u}(s')\,\mathbf{u}(s'):\boldsymbol{\kappa} \qquad \text{(B10)}$$

$$\bar{\nu}(s) = \int_0^L \mathrm{d}s'\,\frac{\partial K(s,s')}{\partial s}\,\mathbf{u}(s')\,\mathbf{u}(s'):\boldsymbol{\kappa} \qquad \text{(B11)}$$

in which $K(s,s')$ is a Greens' function that satisfies

$$\partial^2 K(s,s')/\partial s^2 = -\delta(s - s') \qquad \text{(B12)}$$

subject to boundary conditions $K(0,s') = K(L,s') = 0$. This Green's function is given explicitly[59] by

$$K(s,s') = s\Theta(s' - s) + s'\Theta(s - s') - \frac{ss'}{L} \qquad \text{(B13)}$$

Because the resulting velocity $\bar{\nu}(s)$ depends upon the values of $\mathbf{u}(s')$ at points $s' \neq s$, thus introducing a hierarchy of nonlocal correlation functions into the equations of motion, knowledge of this expression for $\bar{\nu}(s)$ will not allow us to construct explicit solutions for eqs B7 and B8 in general flow histories. It will, however, allow us to treat the linear response to small step deformations in Appendix C, for which the remaining expectation values in eqs B7 and B8 may be evaluated by assuming an equilibrium distribution of chain conformations.

B. Contour Density Fluctuations. We now take into account the slight extensibility of the primitive chain. In the case of a slightly extensible chain, the contour length density ϕ will deviate slightly from its equilibrium value ϕ_{eq}, and, correspondingly, the tangential velocity $\bar{\nu}(s)$ will vary slightly from that given in eq B11. The conservation equation for ϕ in the presence of both an applied macroscopic flow and reptation may be written (after averaging over the stochastic fluctuations of $\nu(s)$ but not over conformations of the chain) as

$$\frac{\partial\phi}{\partial t} - D_{\mathrm{rep}}\frac{\partial^2\phi}{\partial s^2} + \frac{\partial}{\partial s}(\bar{\nu}\phi) = -\phi\boldsymbol{\kappa}:\mathbf{uu} \qquad \text{(B14)}$$

In the limit $|\phi(s) - \phi_{\mathrm{eq}}| \ll 1$, in which we may use the linear approximation of eq 15 for $\mathscr{T}$, this yields a diffusion equation

$$\left[\frac{\partial}{\partial t} - D_\phi\frac{\partial^2}{\partial s^2}\right]\phi \simeq -\phi_{\mathrm{eq}}\boldsymbol{\kappa}:\mathbf{uu} \qquad \text{(B15)}$$

with an effective diffusivity $D_\phi = (B/\zeta) + D_{\mathrm{rep}}$ that reduces to that given in eq 20 in the limit of interest, in which $D_\phi \gg D_{\mathrm{rep}}$. In the limit of an inextensible chain, in which $D_\phi \to \infty$, and/or a slowly varying rate of deformation, we may ignore the time derivative in eq B15 and thereby recover differential eq B9 for $\mathscr{T}(s,t)$.

Appendix C: Small Step Strains

Here we present an outline of the calculation of $\mathbf{F}(\mathbf{u},s)$ and $f(\mathbf{u},s)$ immediately after an infinitesimally small step deformation of an initially equilibrated solution. To do so, we consider a situation in which a constant rate-of-deformation $\boldsymbol{\kappa}$ is applied over a time $\Delta t \ll \tau_{\mathrm{rep}}$ too short for appreciable diffusion to occur. During the

time interval $0 < t < \Delta t$, $f(\mathbf{u},s)$ and $\mathbf{F}(\mathbf{u},s)$ obey differential equations

$$\frac{\partial f}{\partial t} = -\frac{\partial}{\partial \mathbf{u}}\cdot(\mathbf{g}f) + (\kappa:\mathbf{uu})f + \frac{\partial}{\partial s}\langle \bar{v}\hat{f}\rangle \tag{C1}$$

$$\frac{\partial \mathbf{F}}{\partial t} = -\frac{\partial}{\partial \mathbf{u}}\cdot(\mathbf{g}\mathbf{F}) + \mathbf{G}\cdot\mathbf{F}^{\dagger} + \mathbf{F}\cdot\mathbf{G}^{\dagger} + (\kappa:\mathbf{uu})\mathbf{F} + \frac{\partial}{\partial s}\langle \bar{v}\mathbf{ww}\hat{f}\rangle \tag{C2}$$

These equations are obtained from eqs B7 and B8 by dropping the term on the left hand side of each that involves the diffusivity D_{rep} and then rearranging the convective parts by using eq B5 to express $\partial\bar{v}/\partial s$ explicitly. The extra terms $(\kappa:\mathbf{uu})f$ and $(\kappa:\mathbf{uu})F$ on the right hand side of eqs C1 and C2 represent the local stretching or compression of segments by flow, while the remaining terms in brackets describe the effects of connection by the tangential flow.

To calculate the linear response to a deformation, we expand $f(\mathbf{u},s)$ and $\mathbf{F}(\mathbf{u},s)$ to first order in Δt as

$$f(\mathbf{u}) = f^{(0)}(\mathbf{u}) + f^{(1)}(\mathbf{u}) + \ldots$$

$$\mathbf{F}(\mathbf{u}) = \mathbf{F}^{(0)}(\mathbf{u}) + \mathbf{F}^{(1)}(\mathbf{u}) + \ldots \tag{C3}$$

where $\mathbf{F}^{(0)}(\mathbf{u})$ and $f^{(0)}(\mathbf{u})$ are the equilibrium values given in eqs I.17 and I.18 and $f^{(1)}(\mathbf{u})$ and $\mathbf{F}^{(1)}(\mathbf{u})$ are perturbations linear in Δt. The first-order perturbations of f and $\mathbf{F}$ may then be obtained by evaluating the right hand side of eqs C1 and C2 using the equilibrium values of f and $\mathbf{F}$ and using an equilibrium distribution of chain conformations to evaluate the terms involving $\bar{v}$. This calculation is straightforward and yields

$$f^{(1)}(\mathbf{u},s) = \frac{\Delta t}{4\pi}\kappa:(4\mathbf{uu} - \boldsymbol{\delta}) + \Delta t\,\frac{\partial}{\partial s}\langle \bar{v}\hat{f}\rangle_{\mathrm{eq}} \tag{C4}$$

$$\mathbf{F}^{(1)}(\mathbf{u},s) = \frac{\Delta t}{4\pi}\{\kappa + \kappa^{\dagger} + 2\mathbf{uu}(\kappa:\mathbf{uu}) - \mathbf{u}\,(\kappa + \kappa^{\dagger})\cdot\mathbf{u} - \mathbf{u}\cdot(\kappa + \kappa^{\dagger})\mathbf{u}\} + \Delta t\,\frac{\partial}{\partial s}\langle \bar{v}\mathbf{ww}\hat{f}\rangle_{\mathrm{eq}} \tag{C5}$$

where $\langle\ldots\rangle_{\mathrm{eq}}$ denotes an average over the equilibrium distribution of chain conformations.

We now consider the terms of eqs C4 and C5 that depend explicitly on the tangential velocity $\bar{v}(s)$. Focusing first on eq C4 for $f^{(1)}$, we use eq B11 for $\bar{v}(s)$ to write the term of interest explicitly as an integral

$$\frac{\partial}{\partial s}\langle \bar{v}\hat{f}\rangle = \frac{\partial}{\partial s}\int_0^L \mathrm{d}s'\,\frac{\partial K}{\partial s}\kappa:\langle \mathbf{u}(s')\,\mathbf{u}(s')\,\hat{f}(\mathbf{u},s)\rangle_{\mathrm{eq}} \tag{C6}$$

where $K = K(s,s')$ is defined in eq B13. The equilibrium expectation value in the above may be calculated by using the equilibrium correlation function $D(\mathbf{u},\mathbf{u}',|s-s'|)$ defined in Appendix A, giving

$$\langle \mathbf{u}(s')\,\mathbf{u}(s')\,\hat{f}(\mathbf{u},s)\rangle_{\mathrm{eq}} = \int\frac{\mathrm{d}\mathbf{u}'}{4\pi}\,\mathbf{u}'\mathbf{u}'D\,(\mathbf{u}',\mathbf{u},|s-s'|) \tag{C7}$$

Using expansion A2 of D in spherical harmonics, we obtain

$$\langle \mathbf{u}(s')\,\mathbf{u}(s')\,\hat{f}(\mathbf{u},s)\rangle_{\mathrm{eq}} = \frac{1}{12\pi}\boldsymbol{\delta} + \frac{1}{4\pi}(\mathbf{uu} - {}^1/_3\boldsymbol{\delta})\mathrm{e}^{-3|s-s'|/L_{\mathrm{p}}} \tag{C8}$$

where we have used the fact that $\int \mathrm{d}\mathbf{u}\;\mathbf{uu}Y_{lm}(\mathbf{u})$ yields a nonzero result only for $l = 0$ and $l = 2$. By substituting eqs C6−C8 into eq C4, we obtain a total first-order contribution to $f(\mathbf{u},s)$ of

$$f^{(1)}(\mathbf{u},s) = \frac{\Delta t}{4\pi}\kappa:(\mathbf{uu} - {}^1/_3\boldsymbol{\delta})(4 + g(s)) \tag{C9}$$

where

$$g(s) = \frac{L_{\mathrm{p}}}{3L}(\mathrm{e}^{-3s/L_{\mathrm{p}}} + \mathrm{e}^{-3(L-s)/L_{\mathrm{p}}} - 2) \tag{C10}$$

is a function that takes into account the extent to which the value of the velocity $\bar{v}(s)$ is correlated with the orientation $\mathbf{u}(s)$ at the point of interest. The functions g_{end} and $\bar{g}$ appearing in eqs 58 and 128 are defined by

$$g_{\mathrm{end}} \equiv g(L), \quad \bar{g} \equiv \int_0^L \frac{\mathrm{d}s}{L}\,g(s) \tag{C11}$$

i.e., by the value of $g(s)$ at the end of the chain and by the average of $g(s)$.

In the limit $L \gg L_{\mathrm{p}}$ of coil-like chains, the functions $g(s)$, g_{end}, and $\bar{g}$ all vanish, because the self-averaging of $\mathbf{u}(s)$ over the length of the chain causes $\bar{v}(s)$ to vanish in this limit. In the opposite limit $L \ll L_{\mathrm{p}}$ of rod-like chains, the divergence of $\bar{v}(s)$ precisely cancels the local stretching of tube segments, so that the last two terms in the right hand sides of eqs C1 and C2 exactly cancel. In this limit, $g(s)$, g_{end}, and $\bar{g}$ all approach a limiting value of -1. The exact treatment of tangential flow given above is needed to allow the model to reproduce as limiting cases the known numerical prefactors[33] of $G_{\mathrm{link}}(0) = {}^4/_5T$ per link found in the exact treatment of the DE model of flexible entangled coil-like chains and of $G_{\mathrm{link}}(0) = {}^3/_5T$ per rod or link that is found both in models of rigid-rod solutions and in the independent-alignment approximation to the DE model.[33]

Similar reasoning may be used to calculate the remaining term in eq C5. To treat this case, we consider a chain with a constrained value of $\mathbf{u}(s)$ and approximate

$$\langle \mathbf{u}(s')\,\mathbf{u}(s')\,\hat{f}(\mathbf{u},s)\,\mathbf{w}(s)\,\mathbf{w}(s)\rangle_{\mathrm{eq}} \simeq \langle \mathbf{u}(s')\,\mathbf{u}(s')\,\hat{f}(\mathbf{u},s)\rangle_{\mathrm{eq}}\,\frac{1}{L_{\mathrm{p}}a}(\boldsymbol{\delta} - \mathbf{uu}) \tag{C12}$$

This expression is based upon the assumption that, because the equilibrium values of $\mathbf{w}(s)$ are chosen independently for each link from a Gaussian distribution of values within the plane perpendicular to $\mathbf{u}(s)$, there are no significant correlations between $\mathbf{w}(s)\,\mathbf{w}(s)$ and $\mathbf{u}(s')\,\mathbf{u}(s')$ except those imposed by the constraint that $\mathbf{w}(s)$ be perpendicular to $\mathbf{u}(s)$. With this approximation, reasoning similar to that used above to calculate $f^{(1)}(t)$ yields a contribution

$$\frac{\partial}{\partial s}\langle \bar{v}\mathbf{ww}\hat{f}\rangle_{\mathrm{eq}} = \frac{1}{4\pi L_{\mathrm{p}}a}(\boldsymbol{\delta} - \mathbf{uu})\times \{\kappa:(\mathbf{uu} - {}^1/_3\boldsymbol{\delta})g(s) - {}^1/_3\kappa:\boldsymbol{\delta}\} \tag{C13}$$

Because the resulting contribution to $\mathbf{F}^{(1)}(\mathbf{u})$ obeys eq I.18 for the local equilibration of the curvature, however, this term does not contribute the stress $\boldsymbol{\sigma}_{\mathrm{curve}}$. As a result, the function $g(s)$ does not appear in the final result of eq 52 for $G_{\mathrm{curve}}(0)$.

To obtain the linear response of the stress and birefringence to a small step deformation, we substitute the above expressions for $f^{(1)}$ and $\mathbf{F}^{(1)}$ into definitions I.35 and I.36 for $\boldsymbol{\sigma}_{\text{curve}}$ and $\boldsymbol{\sigma}_{\text{orient}}$ and eq 6 for the optical refractive index $\mathbf{n}$. Evaluating the resulting angular integrals then yields eqs 52, 58, and 128 for, respectively, $G_{\text{curve}}(0)$, $G_{\text{orient}}(0)$ and $\mu(0)$.

References and Notes

(1) Morse, D. C. Viscoelasticity of concentrated isotropic solutions of semiflexible polymers. 1. Model and stress tensor. *Macromolecules* **1998**, *31*, 7030.
(2) Sato, M.; Leimbach, G.; Schwarz, W. H.; Pollard, T. D. *J. Biol. Chem.* **1985**, *260*, 8585.
(3) Sato, M.; Schwarz, W. H.; Pollard, T. D. *Nature* **1987**, *325*, 828.
(4) Wachsstock, D. H.; Schwarz, W. H.; Pollard, T. D. *Biophys. J.* **1993**, *65*, 205.
(5) Wachssotck, D. H.; Schwarz, W. H.; Pollard, T. D. *Biophys. J.* **1994**, *66*, 801.
(6) Janmey, P. A.; Hvidt, S.; Peetermans, J.; Lamb, J.; Ferry, J. D.; Stossel, T. P. *Biochemistry* **1988**, *27*, 8218.
(7) Janmey, P. A.; Hvidt, S.; Oster, G..F.; Lamb, J.; Stossel, T. P.; Harwig, J. H. *Nature* **1990**, *347*, 95.
(8) Janmey, P. A.; Euteneuer, U.; Traub, P.; Schliwa, M. *J. Cell Biol.* **1991**, *113*, 155.
(9) Janmey, P. A.; Hivdt, S.; Käs, J.; Lerche, D.; Maggs, A.C.; Sackmann, E.; Schliwa, M.; Stossel, T. P. *J. Biol. Chem.* **1994**, *269*, 32503.
(10) Müller, O.; Gaub, H. E.; Barmann, M.; Sackmann, E. *Macromolecules* **1991**, *24*, 3111.
(11) Ruddies, R.; Goldman, W. H.; Isenberg, G.; Sackmann, E., *Eur. Biophys. J.* **1993**, *22*, 309.
(12) Hinner, B.; Tempel, M.; Sackmann, E.; Kroy, K.; Frey, E. *Phys. Rev. Lett.*, in press.
(13) Ziemann, F.; Radler, J.; Sackmann, E. *Biophys. J.* **1994**, *66*, 2210.
(14) Xu, J. Ph.D. dissertation, Johns Hopkins University, 1997.
(15) Xu, J.; Palmer, A.; Wirtz, D. *Macromolecules* **1998**, *31*, 6486.
(16) Xu, J.; Schwarz, W. H.; Käs, J.; Stossel, T. P.; Janmey, P. A.; Pollard, T. D. *Biophys. J.* **1998**, *74*, 2731.
(17) Amblard, F.; Maggs, A. C.; Yurke, B.; Pargellis, A. N.; Leibler, S. *Phys. Rev. Lett.* **1996**, *77*, 4470.
(18) Gittes, F.; Schnurr, B.; Olmsted, P. D.; MacKintosh, F. C.; Schmidt, C. F. *Phys. Rev. Lett.* **1997**, *79*, 2386. Shnurr, B.; Gittes, F.; MacKintosh, F. C.; Schmidt, C. F. *Macromolecules* **1997**, *30*, 7781.
(19) Käs, J.; Strey, H.; Sackmann, E. *Nature* **1994**, *368*, 226. Sackmann, E.; Käs, J.; Strey, H. *Adv. Mater.* **1994**, *6*, 507.
(20) Käs, J.; Strey, H.; Tang, J. X.; Finger, D.; Ezzell, R.; Sackmann, E.; Janmey, P. A. *Biophys. J.* **1996**, *70*, 1996.
(21) Böhm, J. K. Master's dissertation, University of Texas, Austin, 1997.
(22) Holmes, K. C.; Popp, D.; Gebhard, W.; Kabsch, W. *Nature* **1990**, *347*, 44.
(23) Gittes, F.; Mickey, B.; Nettleton, J.; Howard, J. *J.Cell Biol.* **1993**, *120*, 923.
(24) Ott, A.; Magnasco, M.; Simon, A.; Libchaber, A. *Phys. Rev. E* **1993**, *48*, R1642.
(25) Sato, T.; Teramoto, A. *Adv. Polym. Sci.* **1996**, *126*, 85.
(26) Isambert, H.; Maggs, A. C. *Macromolecules* **1996**, *29*, 1036.
(27) Maggs, A. C. *Phys. Rev. E* **1997**, *55*, 7396.
(28) This estimate of τ_{end} ignores the possible effects of contour length fluctuations. Contour length fluctuations can lead to a more rapid mechanism for randomizing the orientation of the chain ends if the root mean square deviation in the length of the primtive chain exceeds L_p, which (because the primitive chain is nearly inextensible in the regime of interest) occurs only for extremely long chains, of length $L \gtrsim BL_p^2/T \sim L_p(L_p/L_e)^3$. This changes our estimate of τ_{end} in the limit of long chains but reinforces the conclusion that $G_{\text{orient}}(t)$ makes a negligible contribution to $G(t)$ in this limit.
(29) Muthukumar, M.; Edwards, S. F. *Macromolecules* **1983**, *16*, 1475.
(30) Farge, E.; Maggs, A. C. *Macromolecules* **1993**, *26*, 5041.
(31) Gotter, R.; Kroy, K.; Frey, E.; Barmann, M.; Sackmann, E. *Macromolecules* **1996**, *29*, 30.
(32) Kroy, K.; Frey, E. *Phys. Rev. E* **1997**, *55*, 3092.
(33) Doi, M.; Edwards, S. F. *The Theory of Polymer Dynamics*; Oxford University Press: London, 1986.
(34) Odijk, T. *Macromolecules* **1983**, *16*, 1340.
(35) Doi, M. *J. Polym. Sci.: Polym. Symp.* **1985**, *73*, 93.
(36) Semenov, A. N. *J. Chem. Soc., Faraday Trans. 2* **1986**, *86*, 317.
(37) MacKintosh, F. C.; Janmey, P. A.; Käs, J. *Phys. Rev. Lett.* **1995**, *75*, 4425.
(38) The above value for D_ϕ is different, and substantially greater, than that obtained by Isambert and Maggs,[26,27] who obtained a value $D_\phi \sim TL_p/L_e^2$ by requiring the frequency $\omega(q) \sim D_\phi q^2$ of long-wavelength tangential diffusion modes to match the frequency $\omega(q) \sim TL_pq^4/\zeta$ of short-wavelength transverse undulations at a crossover frequency $q \sim 1/L_e$. The "hydrodynamic" argument used here avoids the pitfalls of this matching procedure, since it does not require any assumptions about the nature of the crossover behavior of the coupled longitudinal and transverse modes near $q \sim 1/L_e^{-1}$, which can be shown to be more complicated than that assumed by these authors.
(39) The numerical value of the exponent α has been left undetermined in the above, both for the sake of generality and as a result of some uncertainty on the part of the author regarding the strength of either the thermodynamic self-interaction or the hydrodynamic self-interaction[43] in the limit of interest here. We note only that (i) the effects of both thermodynamic and hydrodynamic interactions must vanish in the limit $d/L_p \rightarrow 0$ in which the polymer becomes a mathematical line and (ii) for any $d/L_p \neq 0$, the effects of both hydrodynamic and thermodynamic self-interactions become stronger with increasing mode wavelength, and so, for chains with $d \ll L_p \ll L$, could conceivably have little effect on high-frequency short-wavelength modes and strong effects on low-frequency long-wavelength modes, leading to a frequency-dependent effective exponent.
(40) Adam, M.; Delsanti, M. *J. Phys. (Paris)* **1982**, *43*, 549; **1983**, *44*, 1185.
(41) Adam, M.; Delsanti, M. *J. Phys. (Paris)* **1984**, *45*, 1513. Roy-Chowdhury, P. V.; Deuskar, D. *J. Appl. Polym. Sci.* **1986**, *31*, 145.
(42) Colby, R. H.; Rubinstein, M. *Macromolecules* **1990**, *23*, 2753.
(43) Bird, R. B.; Curtiss, C.; Armstrong, R. C.; Hassager, O. *Dynamics of Polymeric Liquids*; Wiley-Interscience: New York, 1987; Vol. 2.
(44) Doi, M. *J. Phys. (Paris)* **1975**, *36*, 607. Doi, M.; Edwards, S. F. *J. Chem. Soc., Faraday Trans. 2* **1978**, *74*, 568; **1978**, *74*, 918.
(45) Fixman, M. *Phys. Rev. Lett.* **1985**, *54*, 337; **1985**, *55*, 2429.
(46) Bitsanis, I.; Davis, H. T.; Tirrell, M. *Macromolecules* **1988**, *21* 2824; **1990**, *23*, 1157.
(47) Mead, D. W.; Larson, R. G. *Macromolecules* **1990**, *23*, 2524. Larson, R. G.; Mead, D. W. *J. Polym. Sci., Part B: Polym. Phys.* **1991**, *29*, 1271.
(48) There is a slight approximation made by taking the initial values of $f(\mathbf{u},s,t)$ and $f_{\text{lm}}(s,t)$ to be independent of s, since the tangential flow induced by a small step deformation does introduce a slight s-dependence into the value of $f(\mathbf{u},s,0)$, which is described by eqs C9 and C10. The magnitude of the resulting variation of f with s is, however, found to vanish both when $L \gg L_p$ and when $L \ll L_p$ and is never more than a few percent of the total perturbation of f given in (A7). For simplicity, this slight variation with s has been ignored.
(49) The effective hydrodynamic screening length for an oscillatory undulation mode of wavenumber q in a tightly-entangled solution is actually wavenumber-dependent[26,30,31] and is known to approach a constant value of order $\rho^{-1/2}$ for $q \ll \rho^{1/2}$ but to increase as $\xi_\perp \propto q^{-1}$ for $q \gg \rho^{1/2}$. If we assume that the response at a specified frequency $\omega > \tau_e^{-1}$ is dominated by modes for which the relaxation frequency $\omega(q) \sim \omega$, we find that, for parameters used here to describe actin solutions, $q^{-1} \gtrsim \rho^{-1/2}$ for all $\omega \lesssim 10^4$ rad/s. Since this is near the upper end of the experimentally accessible range, and since $\zeta_\perp$ depends only logarithmically on $\xi_\perp$ and $\xi_\perp \propto q^{-1} \propto \omega^{-1/4}$ at high frequencies, we may treat $\xi_\perp$ as a constant in the frequency range of interest.
(50) Granek, R. *J. Phys. II* **1997**, *7*, 1761.
(51) Gittes, F.; MacKintosh, F. C. *Phys. Rev. E* **1998**, *58*, 1241.
(52) The tube diameter D_{Kas} measured by Käs et al.[19,20] is given by the average of the difference between the maximum and minimum values in a set of 64 values of the normal displacment $h(s)$ relative to the center of the tube, along some direction perpendicular to the tube tangent. Assuming a Gaussian distribution for N randomly chosen values of $h(s)$ yields $D_e \equiv 2[h^2(s)]^{1/2} \simeq 0.5D_{\text{Kas}}$ for $N = 64$.
(53) Hinner, B.; Sackmann, E. Private communication.
(54) Xu, J. Private communication.

(55) Gissler, T.; Weitz, D. *Phys. Rev. Lett.*, submitted for publication.

(56) The power spectral density (PSD) defined by Gittes and Schnurr et al.[18] is actually twice the quantity $\langle|x(\omega)|^2\rangle$ defined here. This difference in convention, which arises from a difference in whether $\langle|x(t)|^2\rangle$ is expressed in terms of an integral of the PSD over all ω (as here) or only over $\omega > 0$ (as in ref 18), has been accounted for in Figure 8.

(57) Isambert, H.; Venier, P.; Maggs, A.; Futtoum, A.; Kassab, R.; Pantaloni, D.; Carlier, M.-F. *J. Biol. Chem.* **1995**, *270*, 11437.

(58) Morse, D. C. Viscoelasticity of concentrated isotropic solutions of semiflexible polymers. 3. Nonlinear rheology. *Macromolecules*, submitted for publication.

(59) Ottinger, H. C. *J. Chem. Phys.* **1990**, *92*, 4540.

MA980304U